The resistivity section consists by three layers except at very shallow layers, a low to medium resistivity layer, a resistive basement and a low to medium resistivity layer which is considered to be a part of the resistive basement. The resistive basement has very high resistivity compared to it of the sections of A-A' to F-F', is very thick and distributed inhomogeneously. A low to medium resistivity part of the resistive basement has wavy shape with variation of resistivity. Especially at around the stations 254 and 301, it appears very deep in the ground.

(8) H-H' Section (see Fig. II-17)

Apparent resistivity in the section is very high compared to the other sections. High and low apparent resistivity appears alternatively in horizontal direction. Resistivity discontinuities are obviously seen at the places between the stations 267 and 270, between the stations 260 and 261, and between the stations 234 and 258.

The resistivity structure of the section generally consists by three layers as the section G-G'. The resistivity distribution at the west of Frizem is inhomogeneous with some resistivity discontinuities. Especially at the shallow part of the stations from 261 to 267, resistivity structure changes drastically and no resistive basement is found.

2-4 Resistivity Structure Map (see PL. II-12 to II-15 and Fig. II-18 to Fig. II-20)

As a result of one dimensional inversions of the all stations, resistivity distribution is illustrated as four plans of 100m, 200m, 500m, and 1,000m of depth from the ground surface.

The general view of the resistivity structure maps are as follows:

i) There are many small resistivity anomalies in the central to the eastern part of the survey area which tend to extend NW-SE direction.

ii) On the other hand, the western part of the survey area is dominated by large resistivity anomalies and high resistivity zones. This means that the resistive basement is generally in the shallow part of the ground.

iii) Very conductivity area is in all depth of the south end of the survey area, the south of Taizelt to the south of Barrage Cavagnac. In the area the resistive basement is very deep and is not found by the current CSAMT survey.

iv) In the preceding section, 2-3, it is explained that resistivity structure which contains Hajar ore deposit is in a concavity of the basement and in many sections the similar structures are found. The similar resistivity structure as it of Hajar ore deposit is found in the following places:

Around Aklij	the stations between 26 and 138
East of Barrage Cavagnac	the stations between 84 and 86
Southeast of Oukhribane	around the station 95

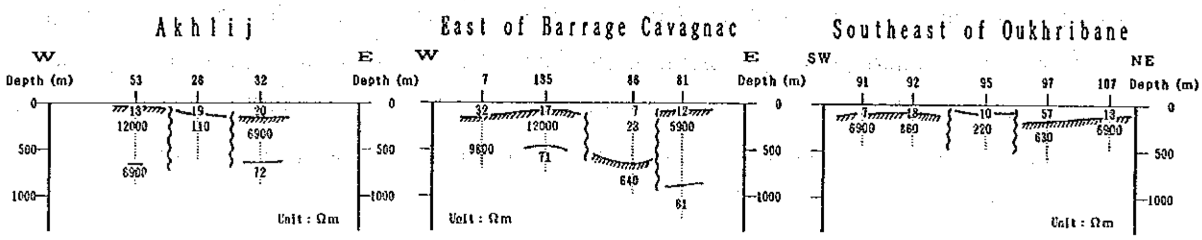

Resistivity distribution of three maps, 100m, 500m, and 1,000m is explained in the following sections:

(1) Resistivity Structure Map (depth 100m) (see PL. II-12 and Fig. II-18)

i) Large blocks of very resistive zones dominate in large area of the map, Taguennza to Tiouli, the west of Hajar mine, the east of Amzourh, Souksou to Taizelt, the east of Khefaouna, and Mkhalif to Arissa. In the resistive zone dominated areas, the resistive basement is assumed to be shallow in the ground.

ii) Conductive zone is as if cutting the aforementioned resistive zones or independently in large resistive zones. The conductive zones are arranged in NW-SE direction.

iii) Many small very conductive anomalies are in the aforementioned conductive zone. Because most of these very conductive anomalies are not seen in the resistivity structure map of 500m deep, they are assumed to be caused by inhomogeneity near the ground surface or under ground water table.

iv) Hajar mine is at the boundary of an extension of a resistive anomaly from the west and a conductive anomaly from the east.

(2) Resistivity Structure Map (depth 500m) (see PL. II-14 and Fig. II-19)

The resistivity distribution of depth 500m is similar to it of depth 100m and changes are as follows:

i) In the western part of the area, the only change is that a conductive zone near Arich in the map of depth 100m becomes resistive in the map of 500m.

ii) Resistivity variations in the central to the eastern part of the survey area in the 100m depth map become small and medium resistivity zones become dominant. Very resistive zones in Taguennza to Tiouli, the west of Hajar mine, Souksou to Taizelt, the east of Khefaouna shrink and only small resistive zones are distributed. Most of very conductive anomalies also disappeared.

iii) Characteristic massive conductive zone surrounded by resistive zones are found at Hajar mine.

(3) Resistivity Structure Map (depth 1,000m) (see PL. II-15 and Fig. II-20)

The resistivity distribution in depth 1,000m is similar to it in depth 500m but resistivity is generally lowered and high resistivity zones become smaller.

A resistive zone in Taguennza to the east of Amzourh disappears and instead conductive zones are arranged in N-S direction. Conductive zones become large in near Taizelt and around Arich.

Tab. II − 2 Rock Properties

No.	Formation	Rock Name	Resistivity (Ωm)	mean	mean	Density (g/cc)	mean	Susceptibility (10^{-5} cgs/emu)	mean
1	Quaternary	Sandstone	61		57	2.27	2.28	3	2
2		〃	53			2.30		2	
3	Permian ~ Carboniferous	Mudstone	240	330	500	2.70	2.71	2	2
4		〃	460			2.73		3	
5		Siltstone	1000	880		2.68		2	
6		〃	780			2.67		2	
7		Carbonatic Schist	550	500		2.73		2	
8		〃	520			2.67		2	
9		〃	670			2.78		2	
10		Pelitic Schist	480			2.76		3	
11		〃	500			2.70		2	
12		〃	420			2.79		3	
13		〃	290			2.65		2	
14		〃	510			2.74		3	
15		〃	690			2.67		1	
16		〃	540			2.67		2	
17		Dacite	230	340		2.73		2	
18		〃	700			2.70		1	
19		〃	250			2.61		3	
20		Quartz vein	1100			2.61		1	
21	Ore of Hajar mine	Pb-Zn-Pyrr. ore	21		15	4.32	4.27	260	530
22		〃	15			4.49		500	
23		〃	14			4.34		1300	
24		〃	11			3.95		480	
	Mean				230		2.88		5

※ mean … Geometrical Average

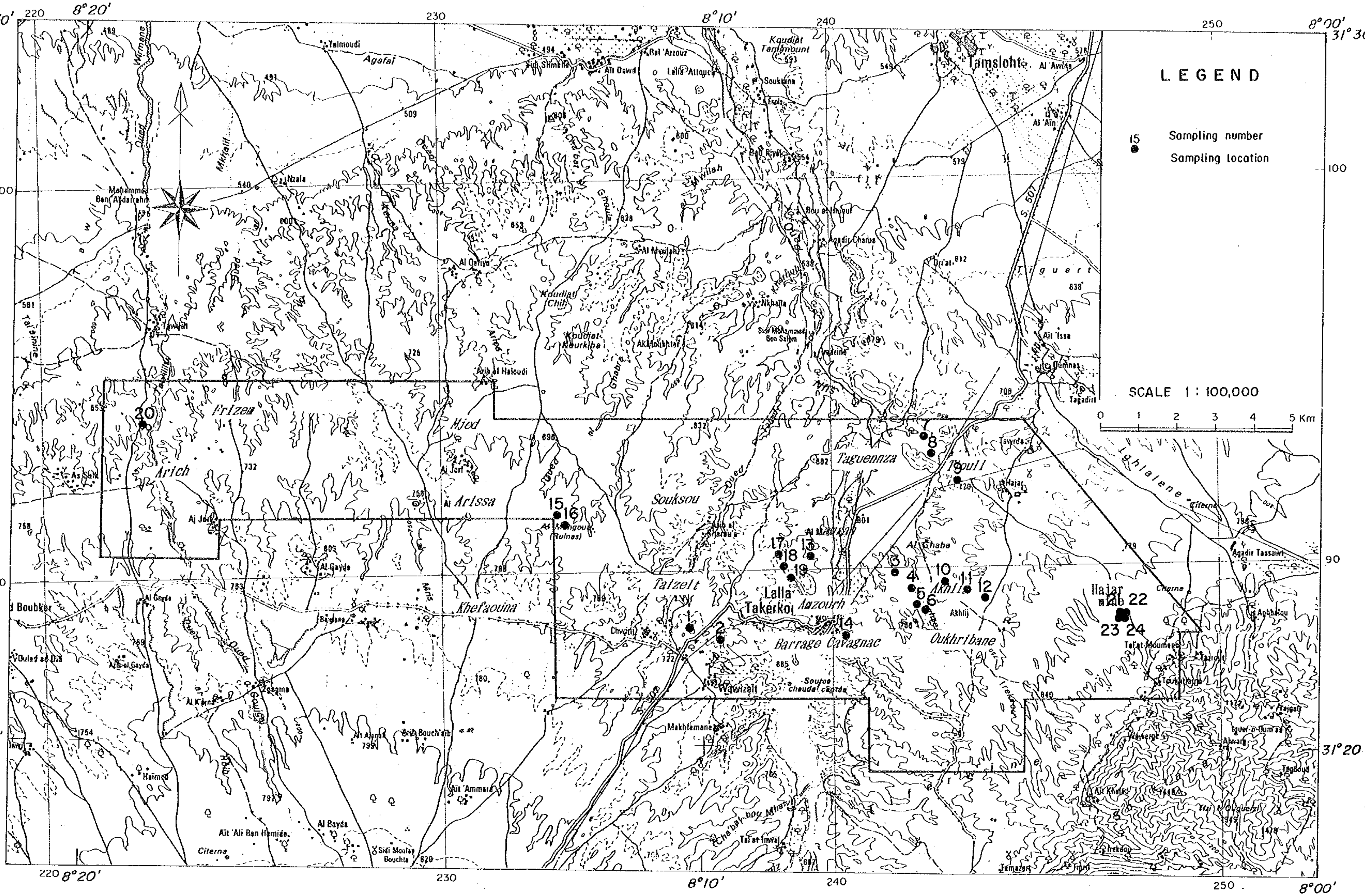

Fig. II-4 Locations of Rock Samples

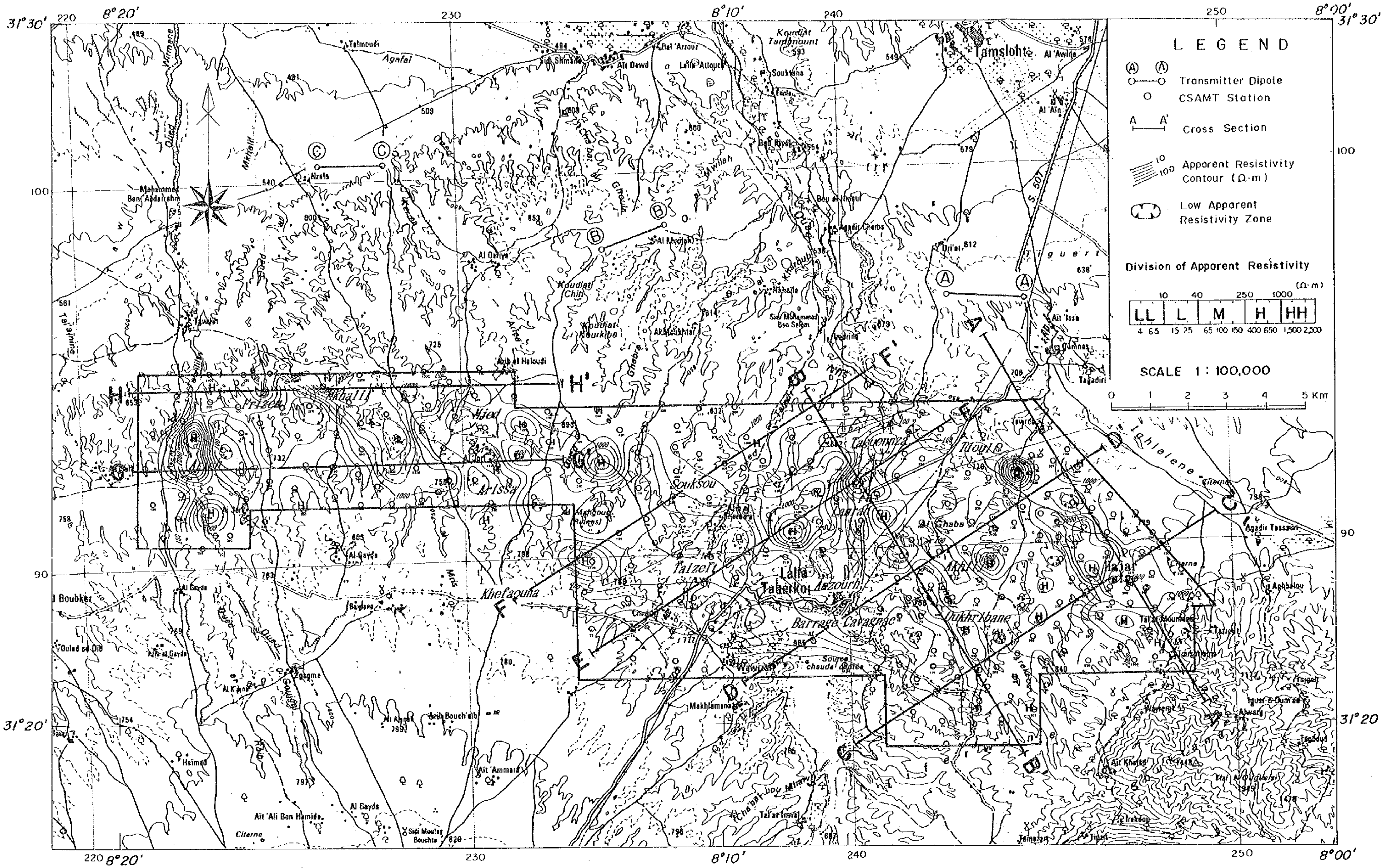

Fig. II-5 Apparent Resistivity Map (Frequency 4Hz)

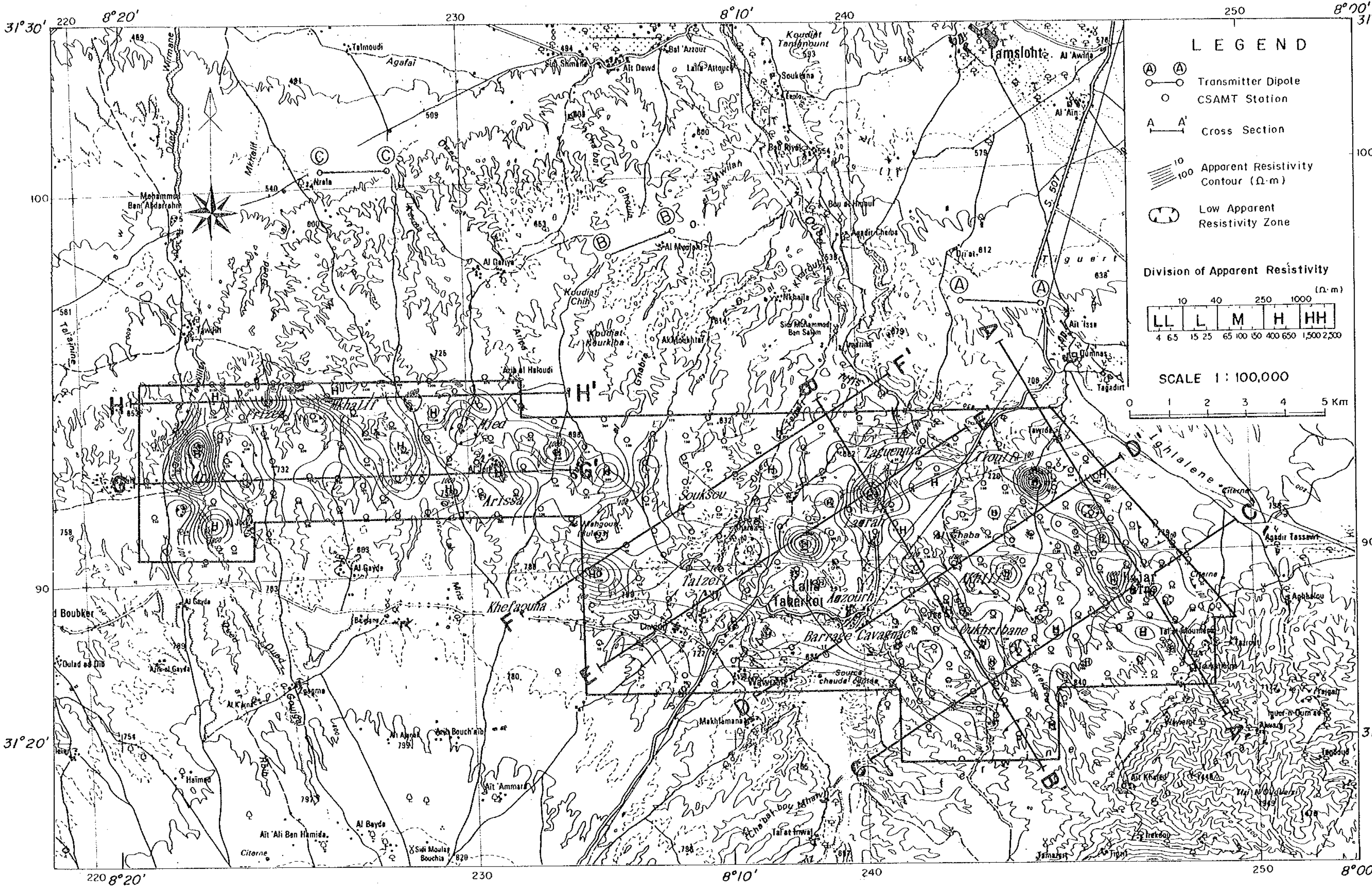

Fig. II-6 Apparent Resistivity Map (Frequency 16Hz)

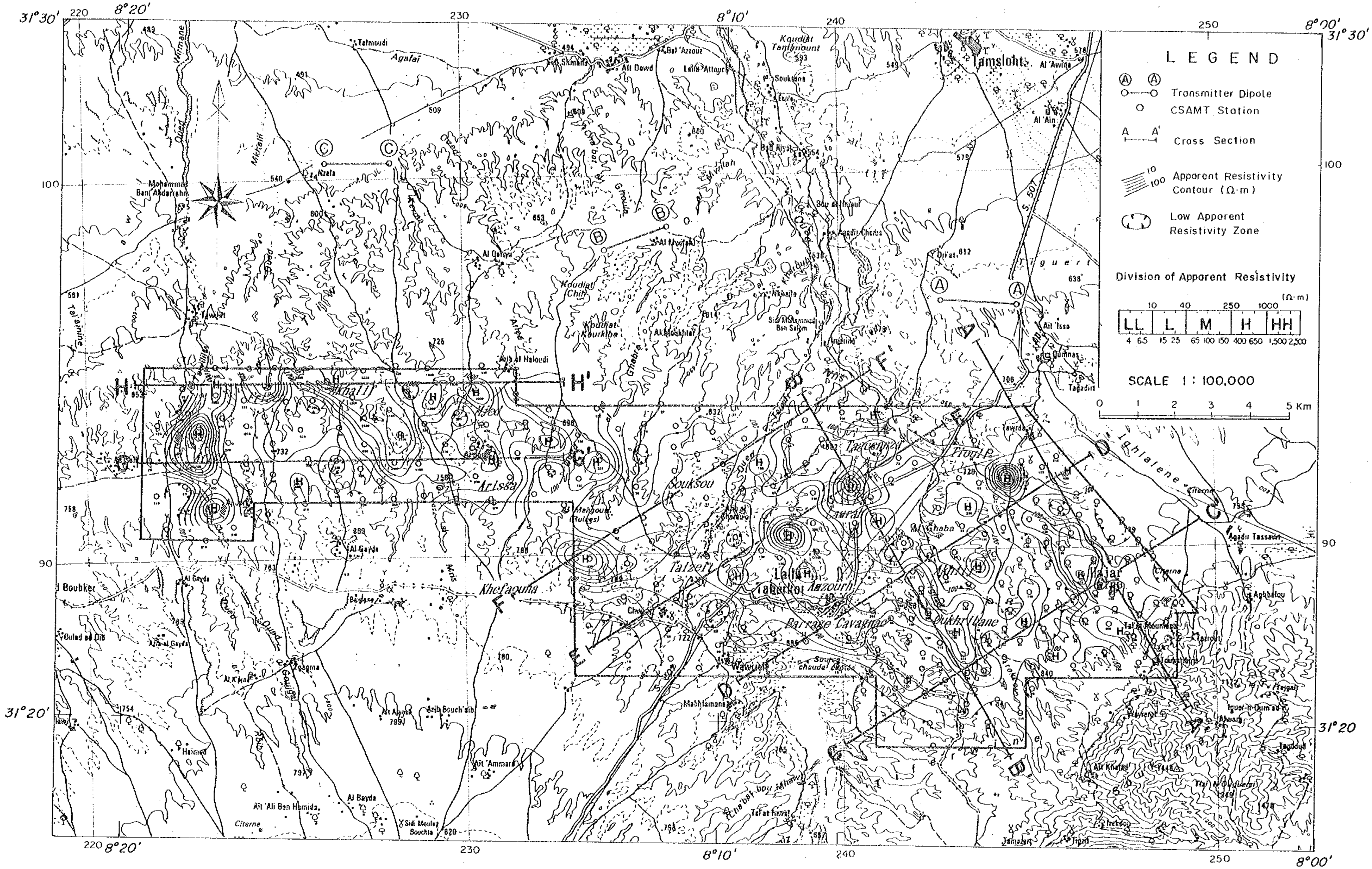

Fig. II-7 Apparent Resistivity Map (Frequency 64Hz)

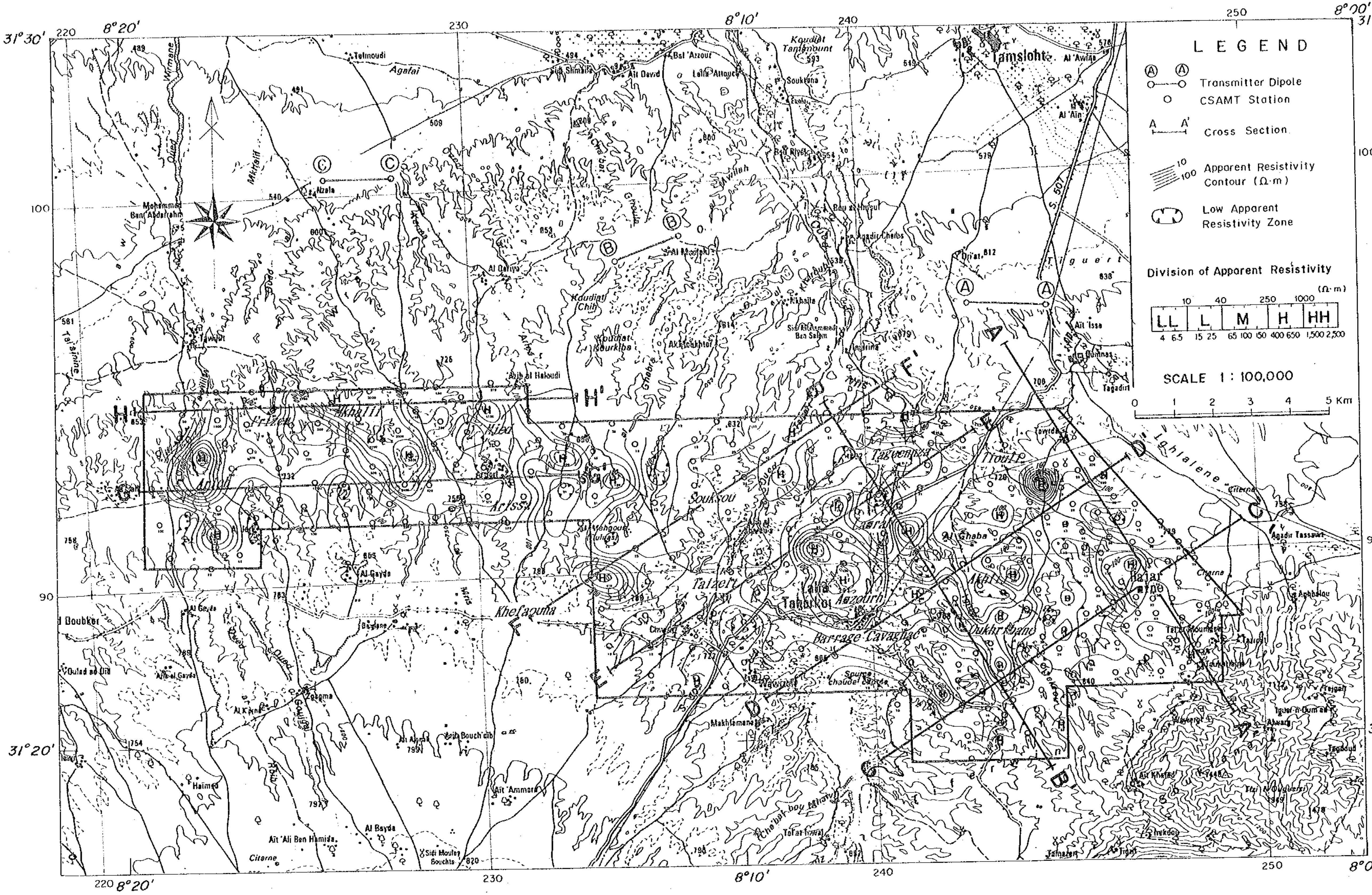

Fig. II - 8 Apparent Resistivity Map (Frequency 256Hz)

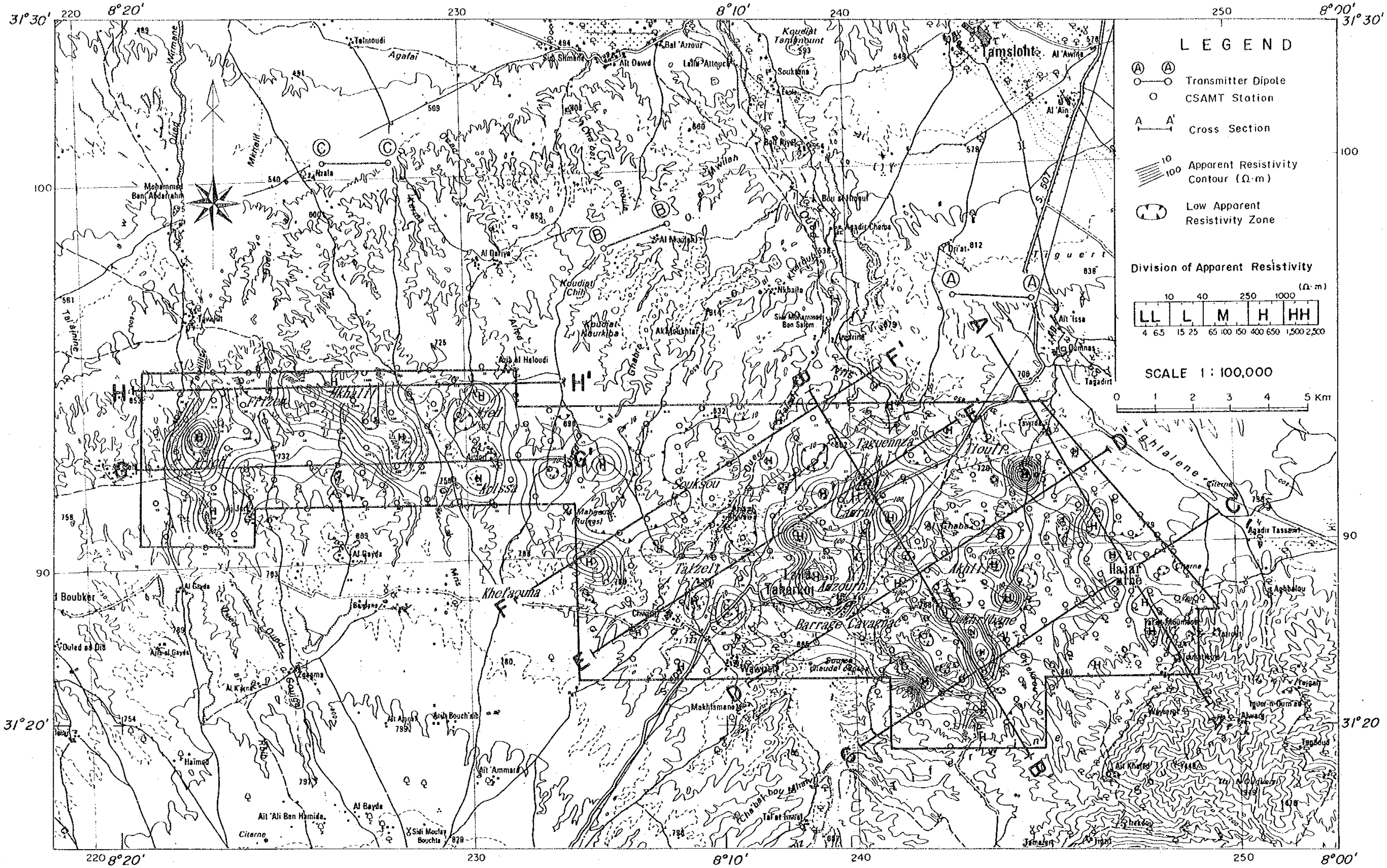

Fig. II-9 Apparent Resistivity Map (Frequency 1,024Hz)

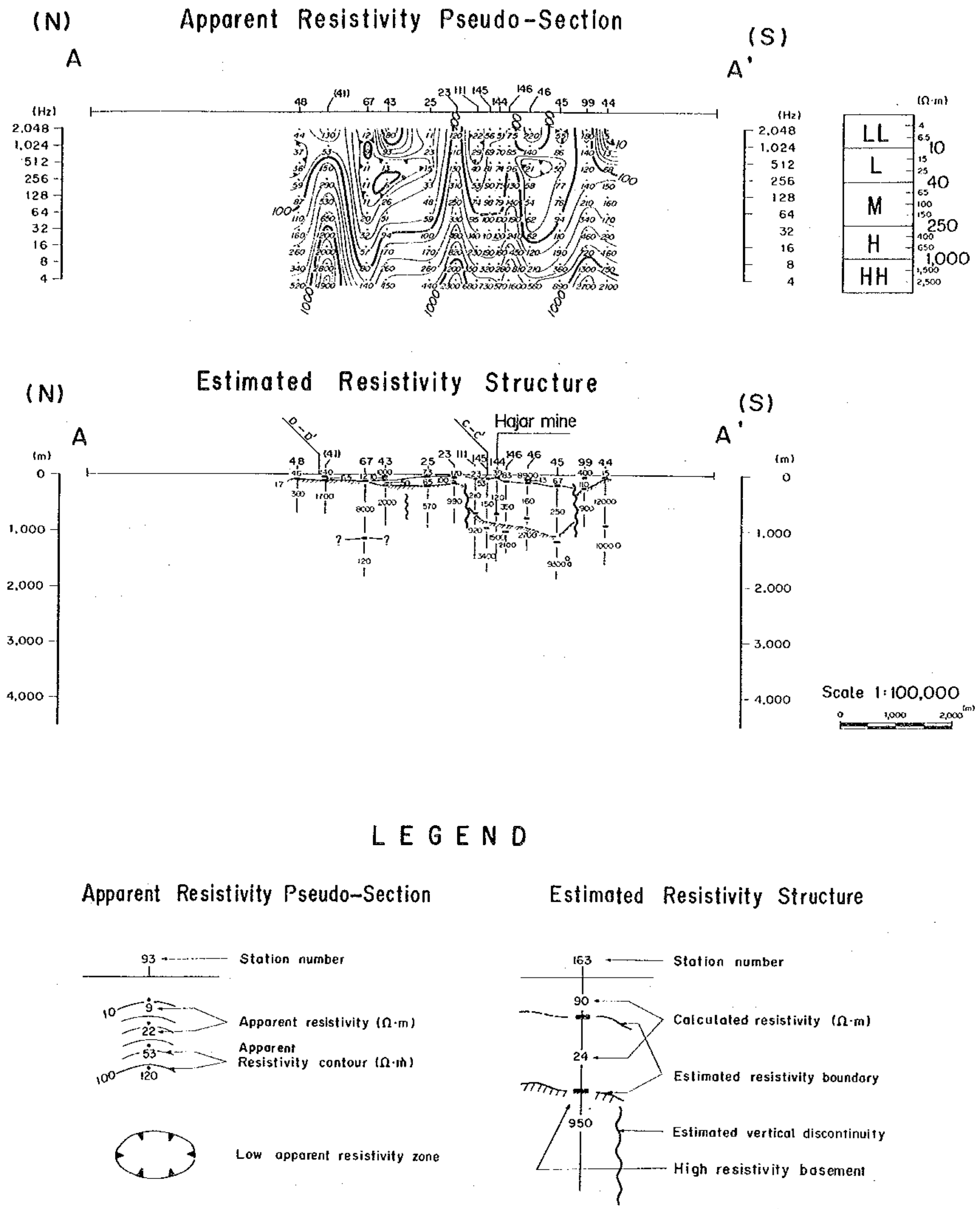

Fig.II-10 Apparent Resistivity Pseudo-Section with Estimated Resistivity Structure (A-A')

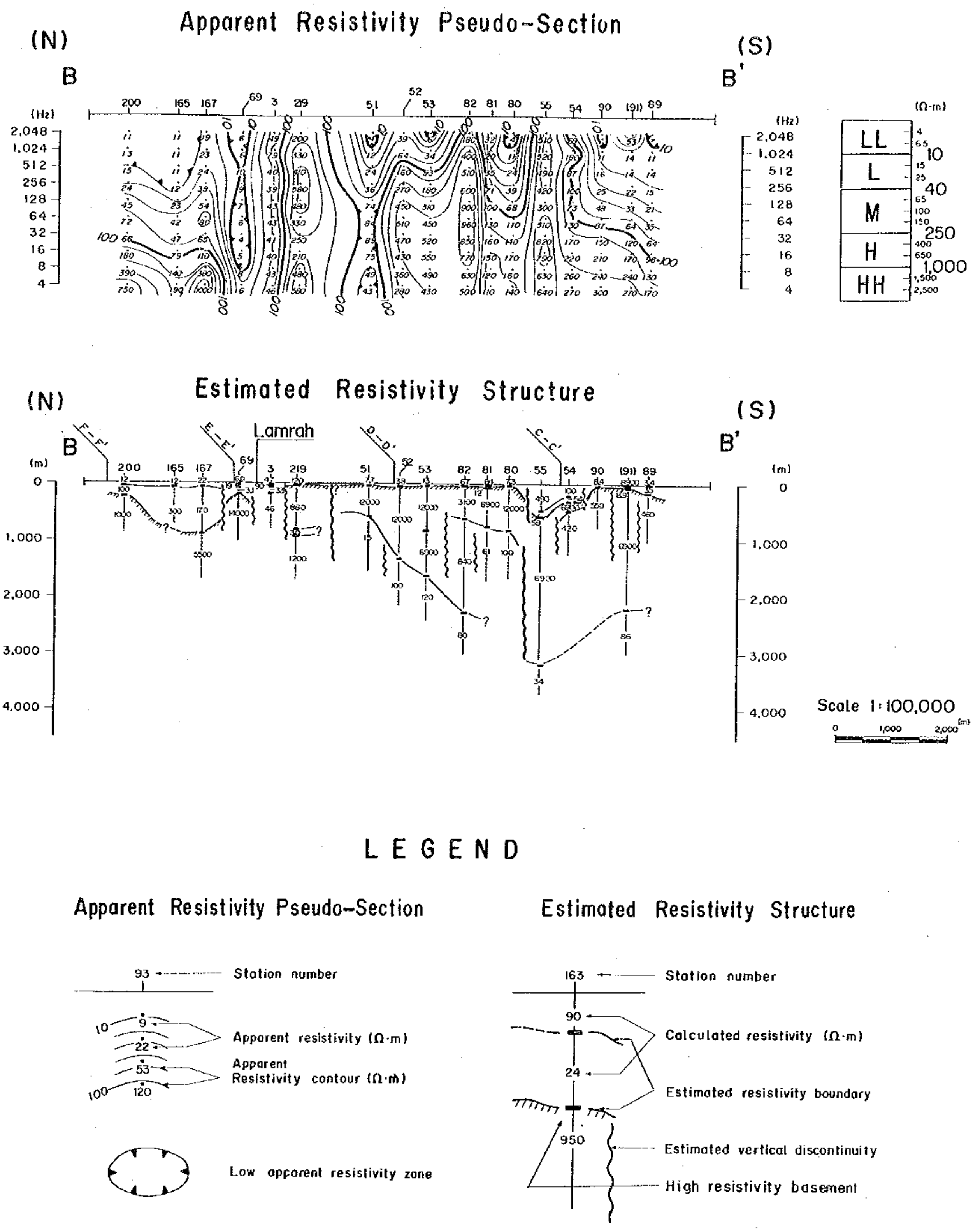

Fig. II-11 Apparent Resistivity Pseudo-Section with Estimated Resistivity Structure (B-B')

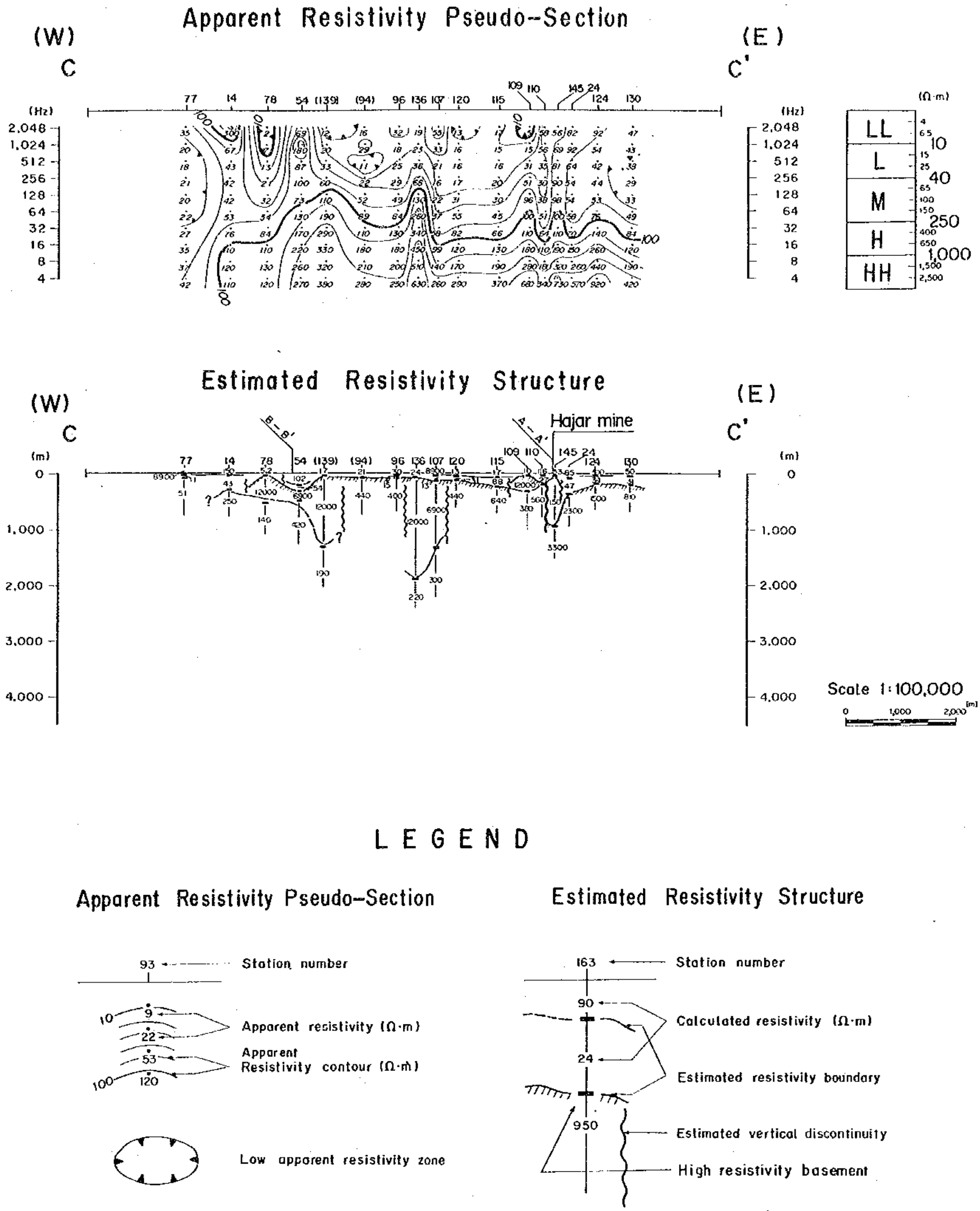

Fig.II-12 Apparent Resistivity Pseudo-Section with Estimated Resistivity Structure (C-C')

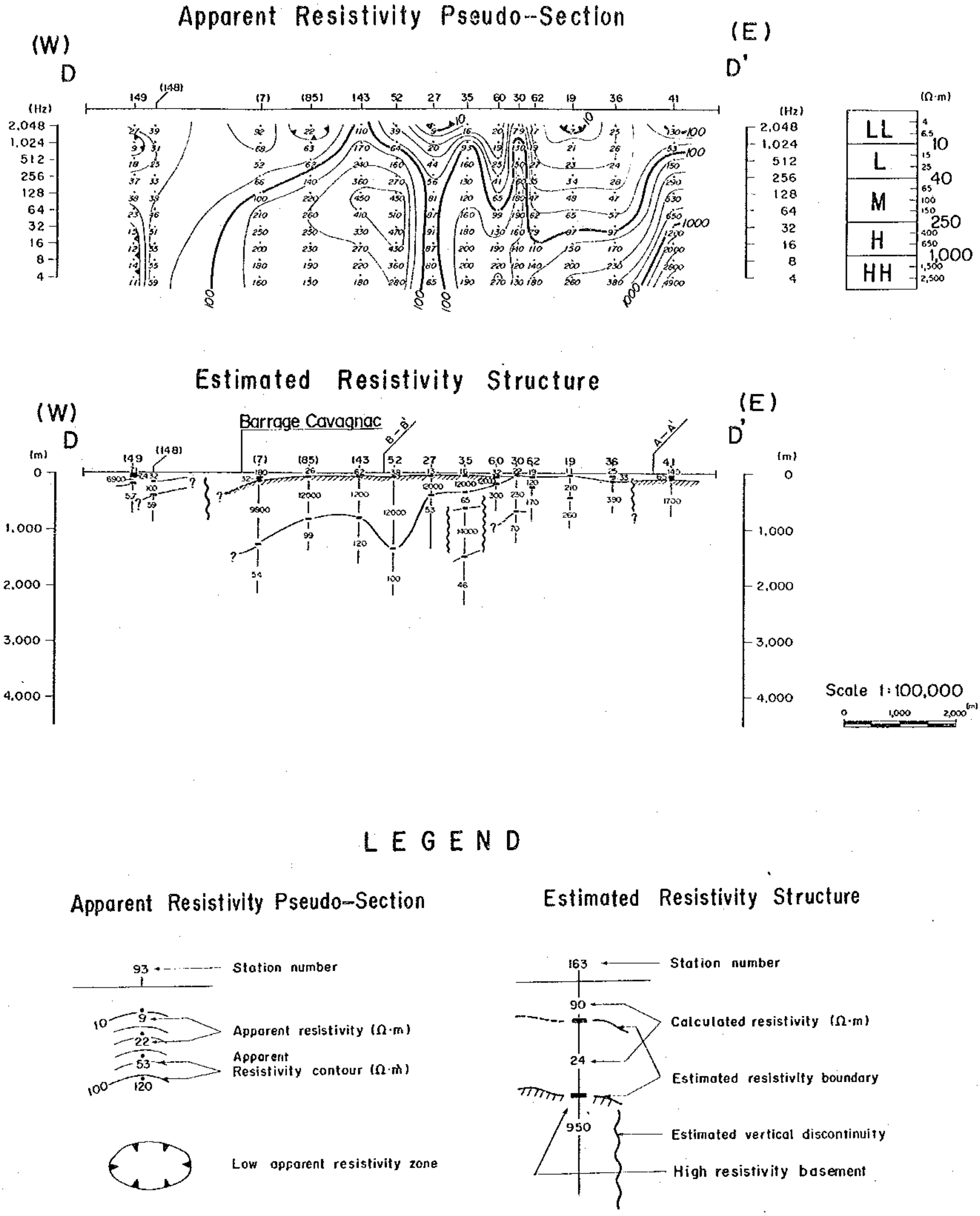

Fig.II-13 Apparent Resistivity Pseudo-Section with Estimated Resistivity Structure (D-D')

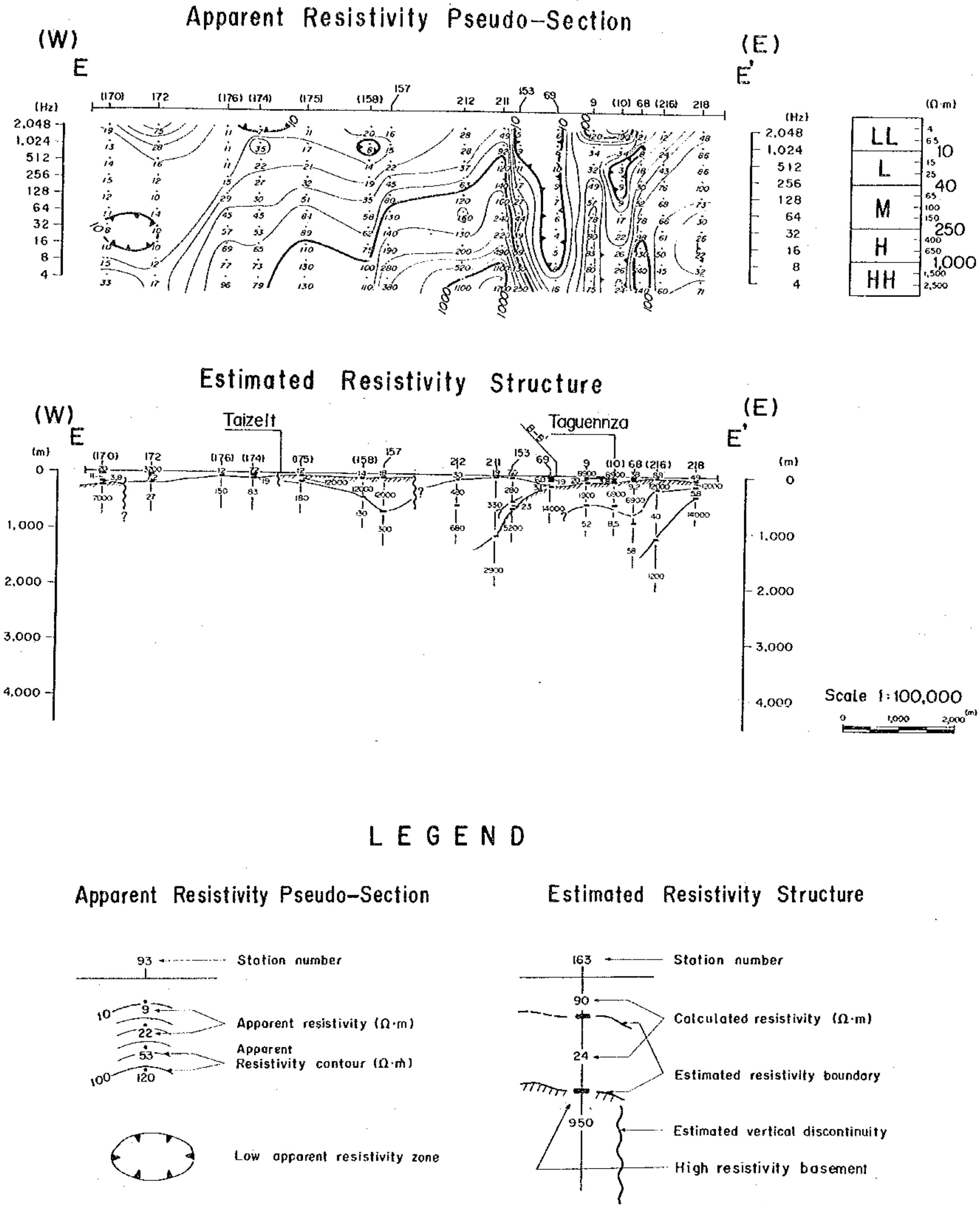

Fig.II-14 Apparent Resistivity Pseudo-Section with Estimated Resistivity Structure (E-E')

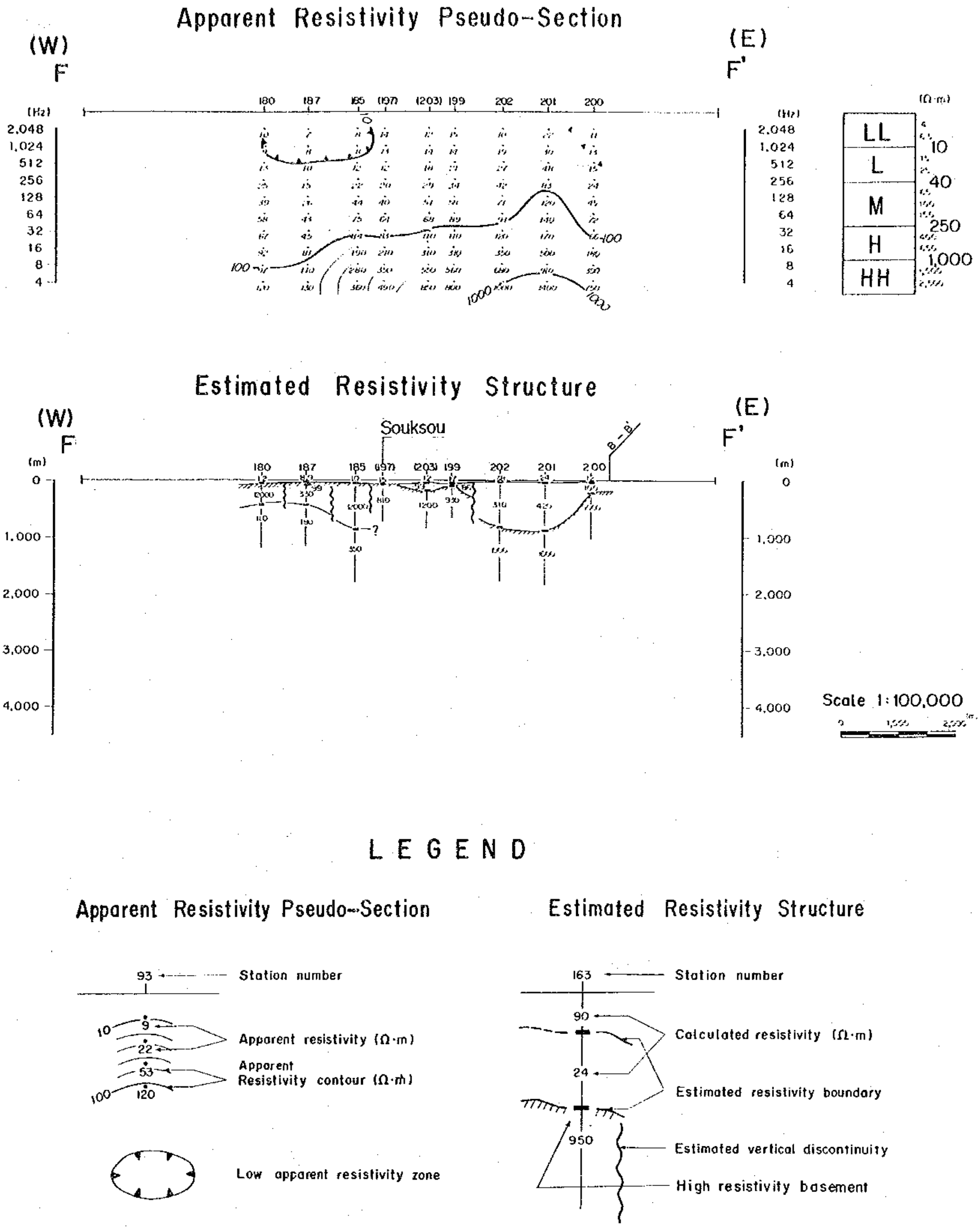

Fig.II-15 Apparent Resistivity Pseudo-Section with Estimated Resistivity Structure (F-F')

Apparent Resistivity Pseudo-Section

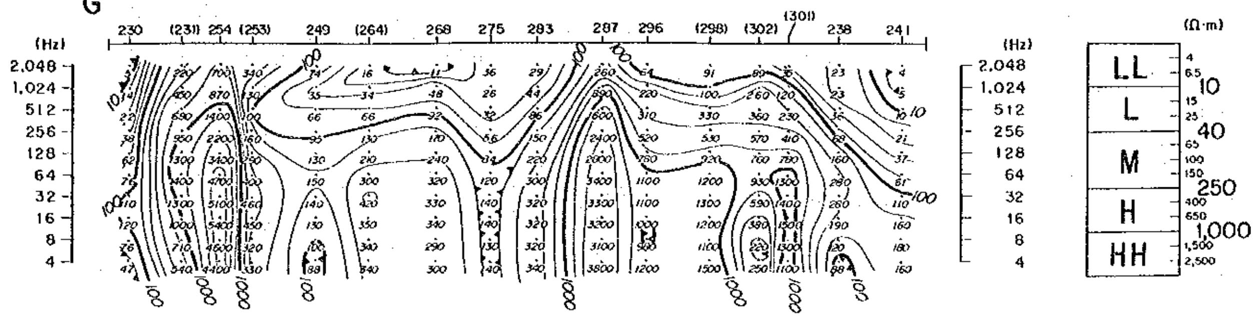

Estimated Resistivity Structure

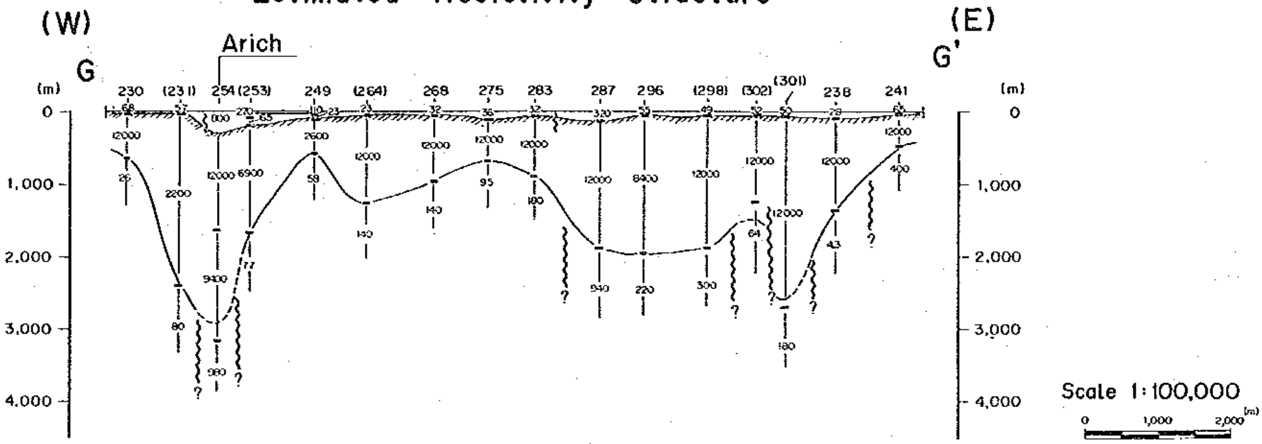

LEGEND

Apparent Resistivity Pseudo-Section

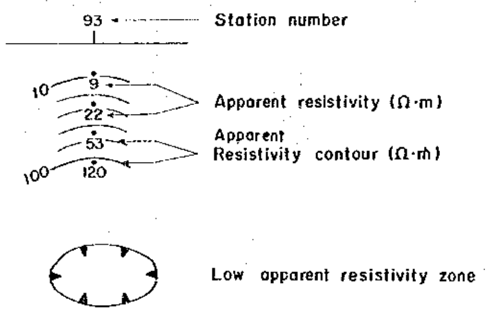

Estimated Resistivity Structure

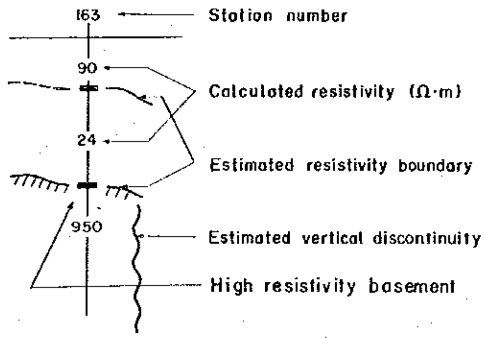

Fig.II-16 Apparent Resistivity Pseudo-Section with Estimated Resistivity Structure (G-G')

Apparent Resistivity Pseudo-Section

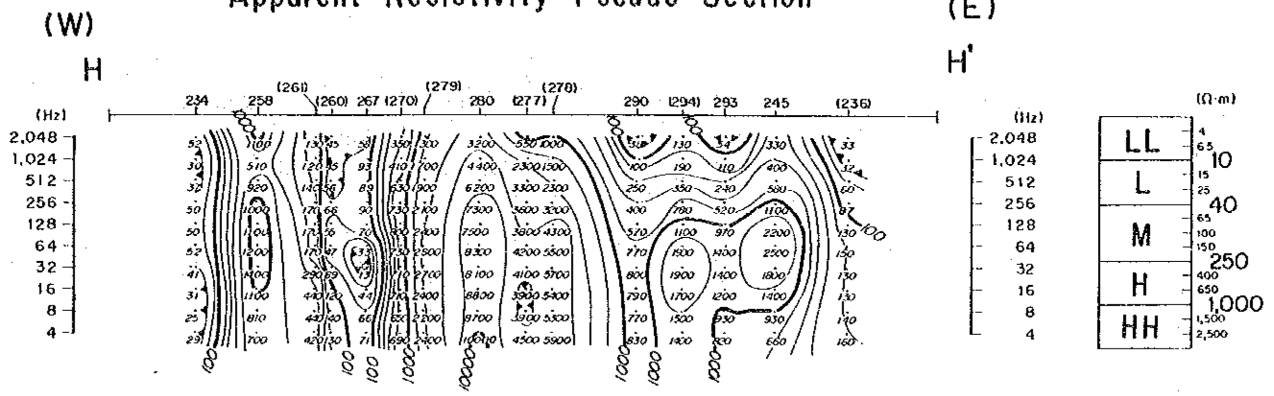

Estimated Resistivity Structure

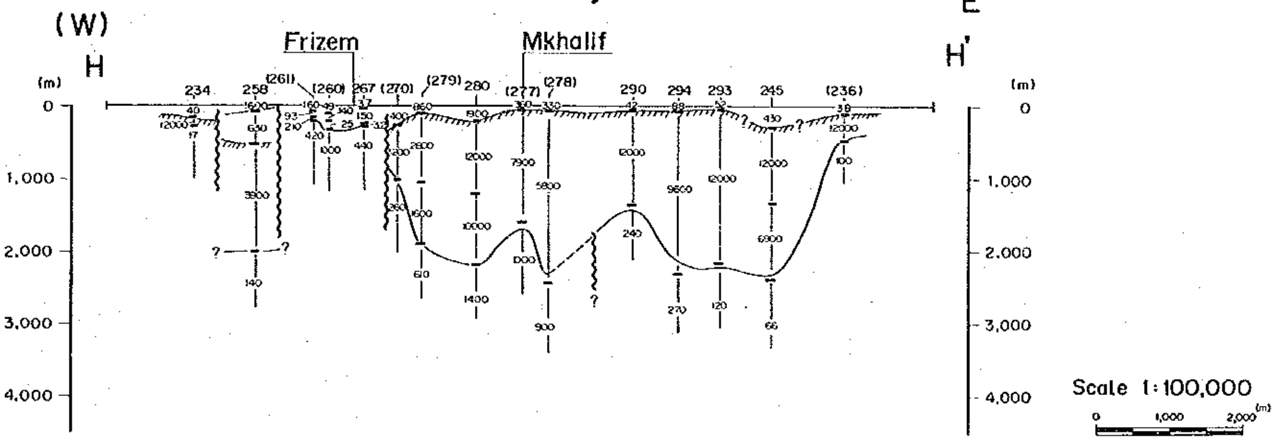

LEGEND

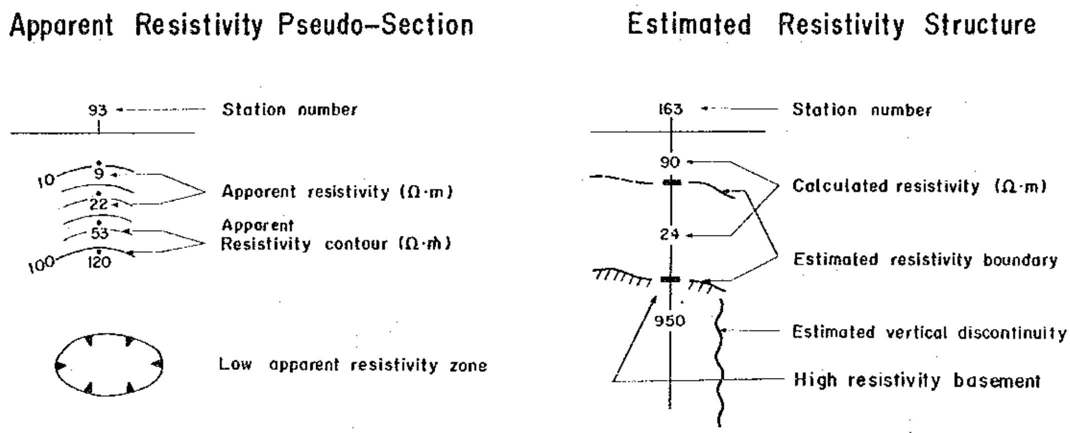

Fig.II-17 Apparent Resistivity Pseudo-Section with Estimated Resistivity Structure (H-H')

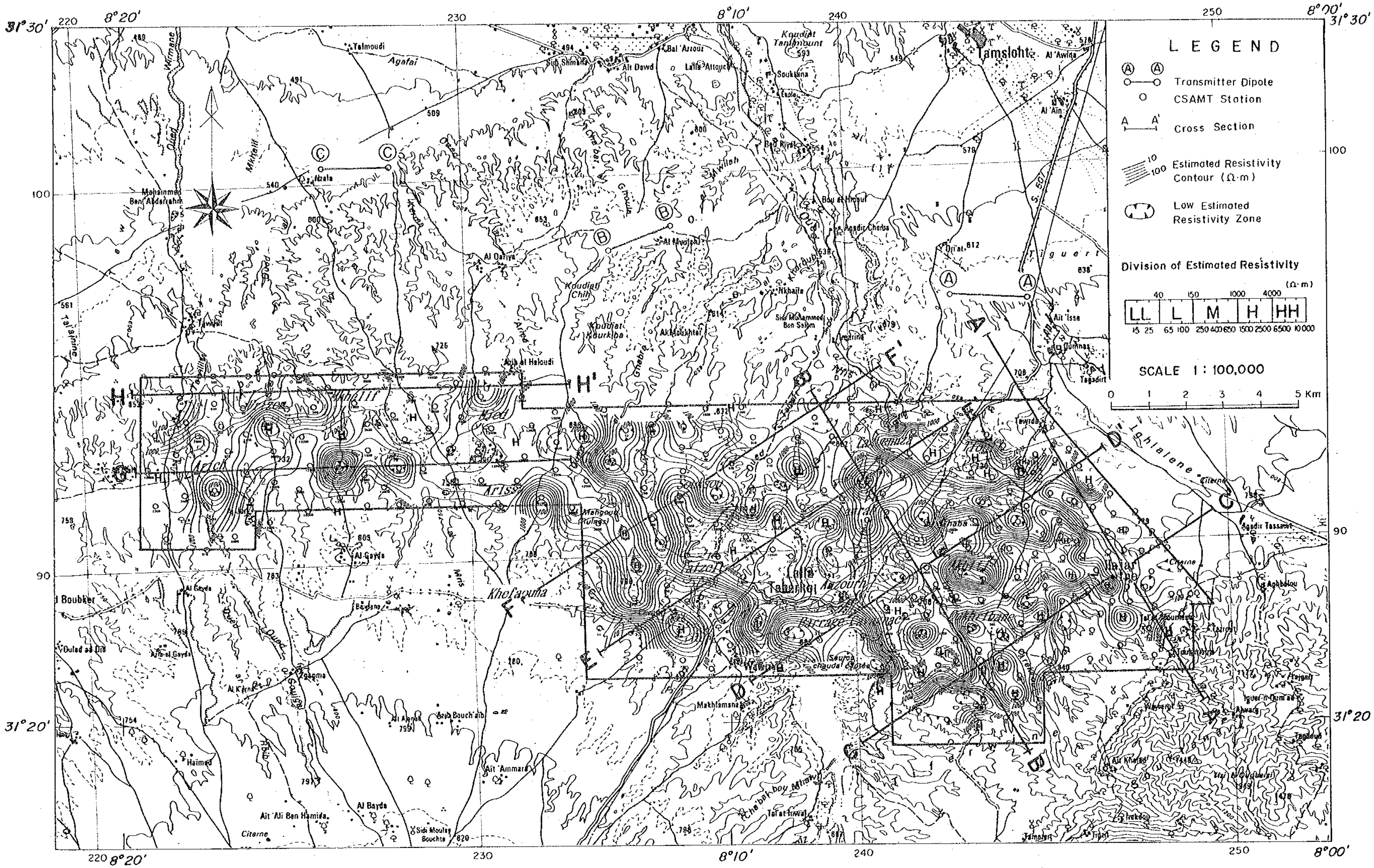

Fig. II-18 Resistivity Structure Map (Depth 100m)

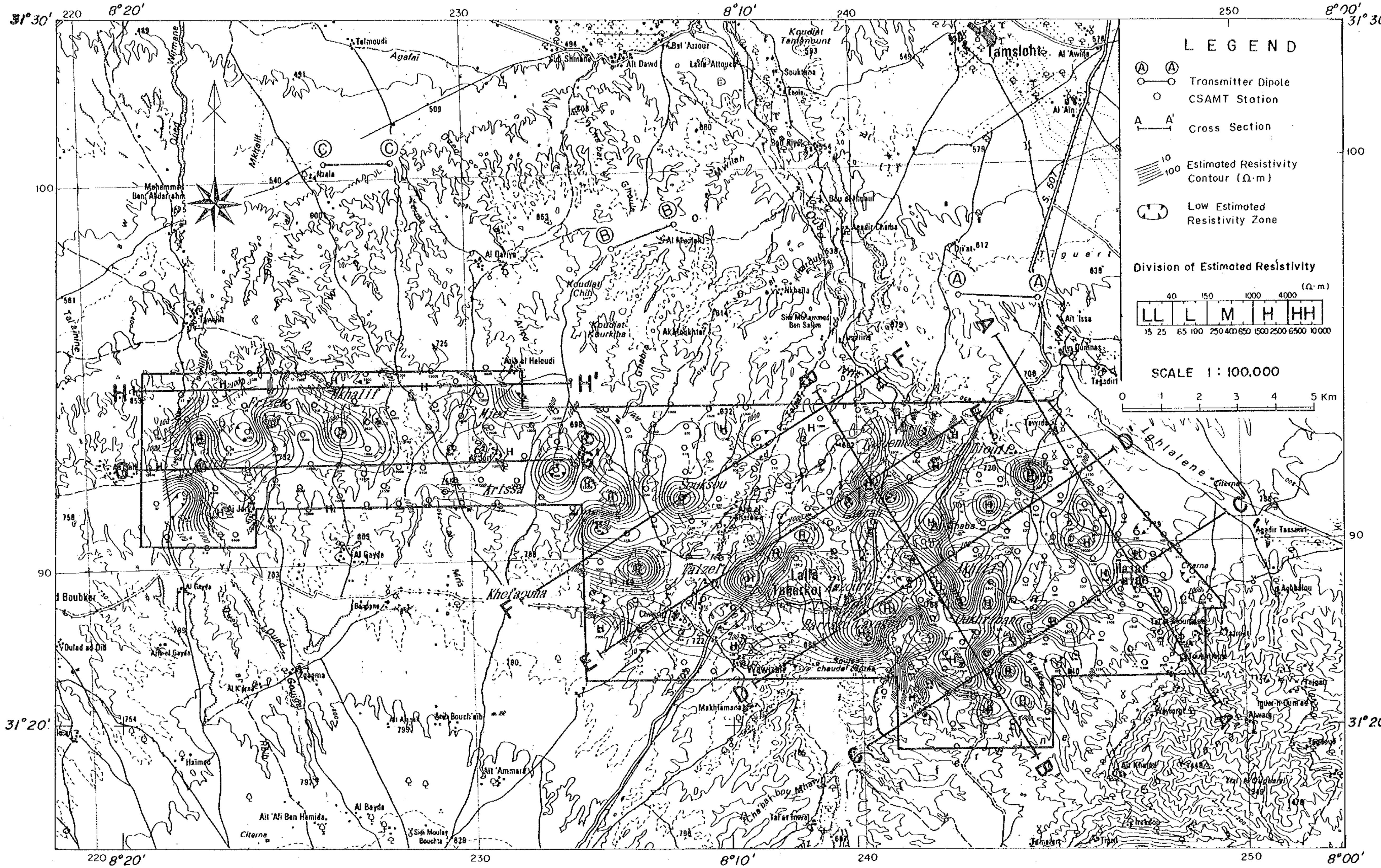

Fig. II - 19 Resistivity Structure Map (Depth 500m)

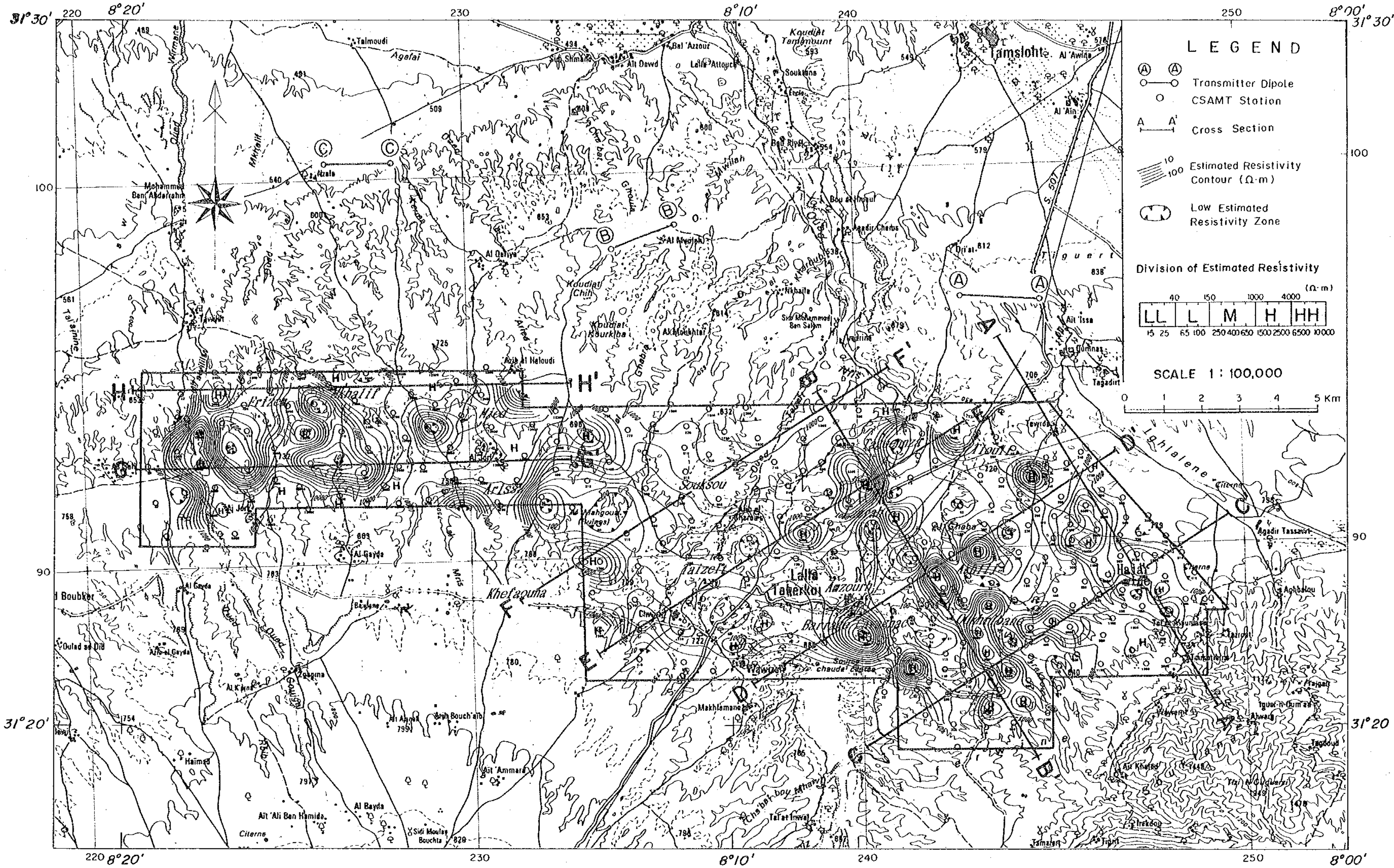

Fig. II - 20 Resistivity Structure Map (Depth 1,000 m)

CHAPTER 3 EXAMINATION

3-1 Resistivity Structure and Geology

The aforementioned resistivity structure is examined against geology of the area (see PL. I-1 and Fig. I-1).

Geological basement of the area is mainly pelitic or calcareous schist or semischist of the Carboniferous and Permian. The Quaternary conglomeratic sandstone overlies the basement.

The basement is scattered in around Tiouli, Akhlij, Oukhribane, Amzourh, and Barrage Cavagnac in the eastern part of the survey area and is distributed widely around Frizem in the western part of the survey area.

Resistivity structure of 100m deep (Fig. II-18) shows very high resistivity corresponding to the area where the geological basement is. It is obvious that the resistivity basement indicates the geological basement of the Carboniferous and Permian. Because conductive anomalies are where the overlying Quaternary is distributed, the Quaternary belongs to a conductive layer. Conductive anomalies are over igneous rocks in the south of Frizem and the south of Barrage Canvagnac.

Resistivity sections (see Fig. II-10 to Fig. II-17) show the resistivity structure in the area consists generally of three layers. The first layer is a conductive layer with resistivity variations which may generally be the Quaternary. The second layer is a very resistive resistivity basement which may be the upper part of the Carboniferous and Permian. The third layer is a relatively low resistivity layer which may be a lower conductive part of the basement.

The geological strike in the area is dominantly NW-SE direction which agrees with distribution of apparent resistivity and resistivity.

3-2 Relation Between Resistivity Structure and Ore Deposits

In the survey area, there are ore indications not only in Hajar mine but gossans in Oukhribane, Amzourh, and Frizem, of which host rock is the basement sedimentary.

Hajar ore deposit is with 100m of the maximum thickness and dips NNE direction. The hanging wall of the deposit is argillized and its foot wall is mostly green rocks. Resistivity measurement of rock samples shows extremely low resistivity of 15Ωm and it was expected that CSAMT might detect the ore deposit as a conductive anomaly. However as the section A-A' (Fig. II-10), the mineralized alteration zone is detected as a conductive anomaly in (or a concave of) the resistive basement.

When we see the ore indications in Oukhribane, Amzourh, and Frizem on the resistivity structure maps, the ore indications are in conductive anomalies next to resistive areas which is similar locations to Hajar ore deposit.

3-3 Examination of the Existing Informations and Comparison with Resistivity Structure

The area has been studied by magnetic survey, gravity survey, air-borne electromagnetic survey and other geophysical survey. Among them, the following figures are attached on the report.

Air-borne magnetic survey (Fig. II-21)

Regional gravity survey (Fig. II-22)

Detailed magnetic survey over Hajar mine (Fig. II-23)

Detailed gravity survey over Hajar mine (Fig. II-24)

(1) Air-borne Magnetic Survey (see Fig. II-21)

Residual magnetic anomalies show quite different distribution on the western part and the center to eastern part of the survey area.

Magnetic anomalies in the eastern part of the survey area are combinations of low anomaly in the north and high anomaly in the south, like anomalies over Hajar mine, which are typical response from a buried magnetic sphere model, and in the east of Barrage Cavagnac. Magnetization of the area has the same polarization as the earth.

On the other hand most magnetic anomalies in the western part of the survey area are mostly positive ones. Therefore there must be remnant magnetization with different directionality of the present earth. The background magnetic intensity in the western area is several tens of gammas more than the central to the eastern part of the survey area.

Therefore, magnetic bodies in the western part of the survey area and in the central to the eastern part of the survey area are thought to have been formed in different geological age, and geomagnetic basements of the both areas are also thought to be different.

Extremely high magnetic anomalies , which are similar to them in the western part of the survey area, are distributed in the south of Daoud and the south of Rial which are north of the geophysical survey area.

The following relations are found between magnetic anomalies and geological structure:

i) Magnetically anomalous bodies which are inferred from airborne magnetic map are mostly at concaves of resistivity structure, which are conductive anomalies surrounded by resistive zones in the resistivity structure maps(see Fig. II-18 to Fig. II-20). Their typical examples are magnetically anomalous bodies, around Hajar mine, the south of Oukhribane, around Taguennza, the west of Frizem. Resistive anomaly is found at magnetic anomalies around Mjed.

ii) Scattered small anomalies are seen in the eastern part of the survey area on the apparent resistivity maps and the resistivity structure maps and are arranged in NW-SE direction. The same tendency is found in the airborne magnetic anomalies.

iii) In the central part of the survey area centered by the area from Souksou to Taizelt, there are not so much change in apparent resistivity values, resistivity structure and airborne magnetic values.

iv) Resistive basement in the western part of the survey area is very shallow in the ground and is quite different from it in the central to the eastern part. The fact is harmonious with the aforementioned fact that the magnetic basement in the both areas are different.

(2) Regional Gravity Map (see Fig. II-22)

Fig. II-22 is a regional gravity map with station density of 1.3/square km. Gravity is high in the western part, decreases toward the east and drops drastically in the south. The gravity basement is shallow in the western part of the survey area, increases its depth toward the east and subsides with a thick low-density layer in the southern part of the survey area.

Gravity anomalies are related to resistivity anomalies as follows:

i) The shallow resistive basement with rather homogeneous resistivity in the western part of the survey area corresponds to high gravity anomaly distribution.

ii) High gravity anomaly extends to NW-SE direction in the eastern to central part of the survey area. The NW-SE extensions of the high gravity anomalies correspond to distributions of high apparent resistivity and resistive zones of resistivity structure and are harmonious with general trend of structure in the area, NW-SE direction.

iii) Very low gravity zone at the south end of the survey area corresponds to very low apparent resistivity and very conductive zone. This zone is thought to be very thick conductive Quaternary filled with large amount of underground water overlying on the basement.

(3) Detailed Magnetic and Gravity Survey over Hajar Mine (see Fig. II-23 and Fig. II-24)

The results of detailed magnetic and gravity survey with station interval of 25m are illustrated in Fig. II-23. The section crossing Hajar mine is illustrated with resistivity structure and geological section (see Fig. II-24).

The ore body rich in pyrrhotite is clearly detected by the detailed magnetic survey and the detailed gravity survey detected the dense ore deposit (see Tab. II-2) as high gravity anomaly.

Resistivity zoning is shown in Fig. II-24 as L, M, H and HH. The relations between resistivity zoning and geology are as follows:

Resistivity zoning	Resistivity	Relation with geology and deposit
L	about 50 Ωm	Correlated to Quaternary. Thickness is several hundred meters.
M	about 150 Ωm	Correlated to Hajar ore deposit, the argillized hanging wall and the foot wall of green rock. Accompanying to mineralization, host rock originally resistive became conductive.
H and HH	400 to 4,000 Ωm	Correlating to resistive basement without mineralization and alteration.

The resistivity zone, M, extends to the southeast of the Hajar mine (see Fig. II-10 and Fig. II-19) where high gravity anomaly also extends. The southeast extension of Hajar mine is a prospective ore bearing zone.

3-4 Conclusion

Hajar ore body represents ore deposits in the area and its ore is high magnetic permeability, high density, and conductive as stated in Rock Property (Tab. II-2). However, for the current CSAMT survey, Hajar ore body was not detected independently as a conductive zone but the ore body and the surrounding altered zone were detected as a single conductive zone.

The conductive zone which indicates Hajar ore body is surrounded by resistive area, namely a concave in the basement, Carboniferous and Permian.

The CSAMT survey found many conductive anomalies. Some of the conductive anomalies may be caused by underground water. The Quaternary widely covering the survey area consists mainly by conglomeratic sandstone and contains shallow aquifer. Shallow aquifers in the area may also be detected as conductive zones. Therefore, conductive zones must be interpreted with a great circumspection to discriminate aquifers from concaves of the resistive basement which may indicate ore bodies.

Conductive zones at near the ground surface and horizontally continuous or very inhomogeneous structure are considered to be influenced by aquifer and are listed as follows:

i) The north to the east of Hajar mine: see the stations from 25 to 67 on Fig. II-10.

ii) The east to the southeast of Oukhribane: see the stations 96 to 115 on Fig. II-12.

iii) The southeast of Khefaouna - the south of Barrage Cavagnac -south of Oukhribane: see the west end of Fig. II-12, II-13 and II-14.

iv) The south of Taguennza: see the stations 10 to 69 of Fig. II-14.

v) Around and the north of Souksou: see the stations 180 to 199 of Fig. II-15.

Conductive anomalies which are thought to be concaves in the resistive basement and to be related to mineralization except those aforementioned are as follows (see Fig. 3).

conductive zone	location (station)	relation to other geophysical data	Fig.No.
Near Hajar mine	45-111 -108	very high magnetic and high gravity anomaly	II-10 II-19
Southeast of Souksou	201-202	small high magnetic anomaly	II-15
West of Taguennza	165-167		II-11
Near Lamrah	3-153	small high magnetic anomaly	II-11 II-19
Near Akhlij	26-138	small high magnetic anomaly	II-18 II-19
East of Barrage Cavagnac	84- 86	deep magnetic body	II-19 II-20
Southeast of Oukhribane	95		II-19 II-20
South of Oukhribane	54,55-93	remarkable magnetic anomaly	II-11 II-19
West of Frizem	256-260	very high magnetic anomaly	II-17 II-18

All of the aforementioned conductive anomalies except on Hajar mine and the west of Frizem are in the zone of 3km wide extending in NW-SE direction from the west of Taguennza, Lamrah, to Oukhribane (see Fig. 3). In the other words, the conductive zones in the same horizon as

Hajar ore deposit in the aforementioned zone are highly prospective zone for ore deposits.

The current CSAMT survey is a regional survey to study large geological structure in the survey area. The results of the CSAMT survey show the basement structure and resistivity environment of mineralization and the survey has accomplished its original aim.

We recommend that the aforementioned extracted conductive zones as highly prospective zones except around Hajar mine, which has been studied in details, must be studied in details by a method which can clarifies difference of physical properties of ore and host rocks.

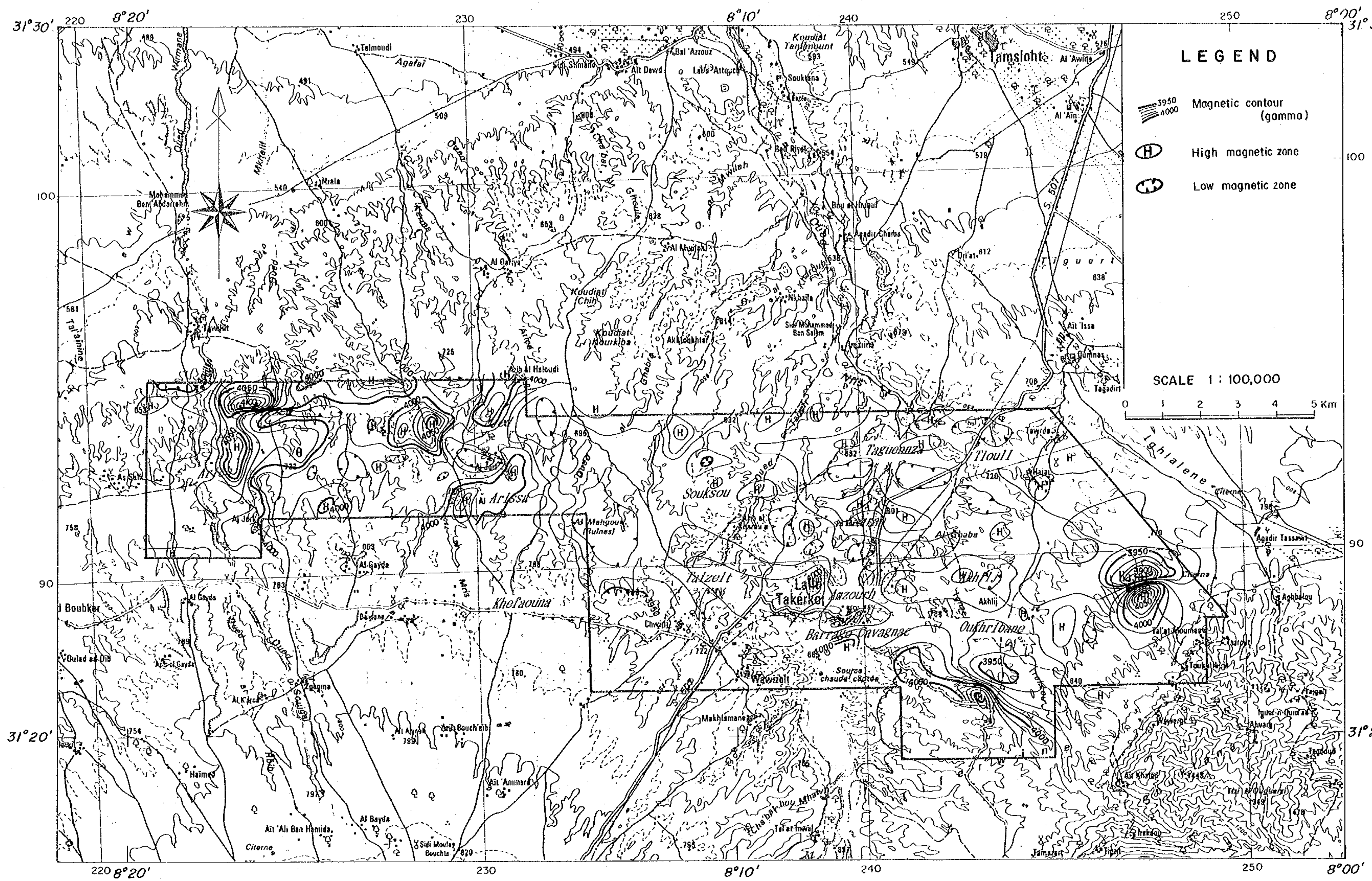

Fig. II-21 Residual Airborne Magnetic Anomalies

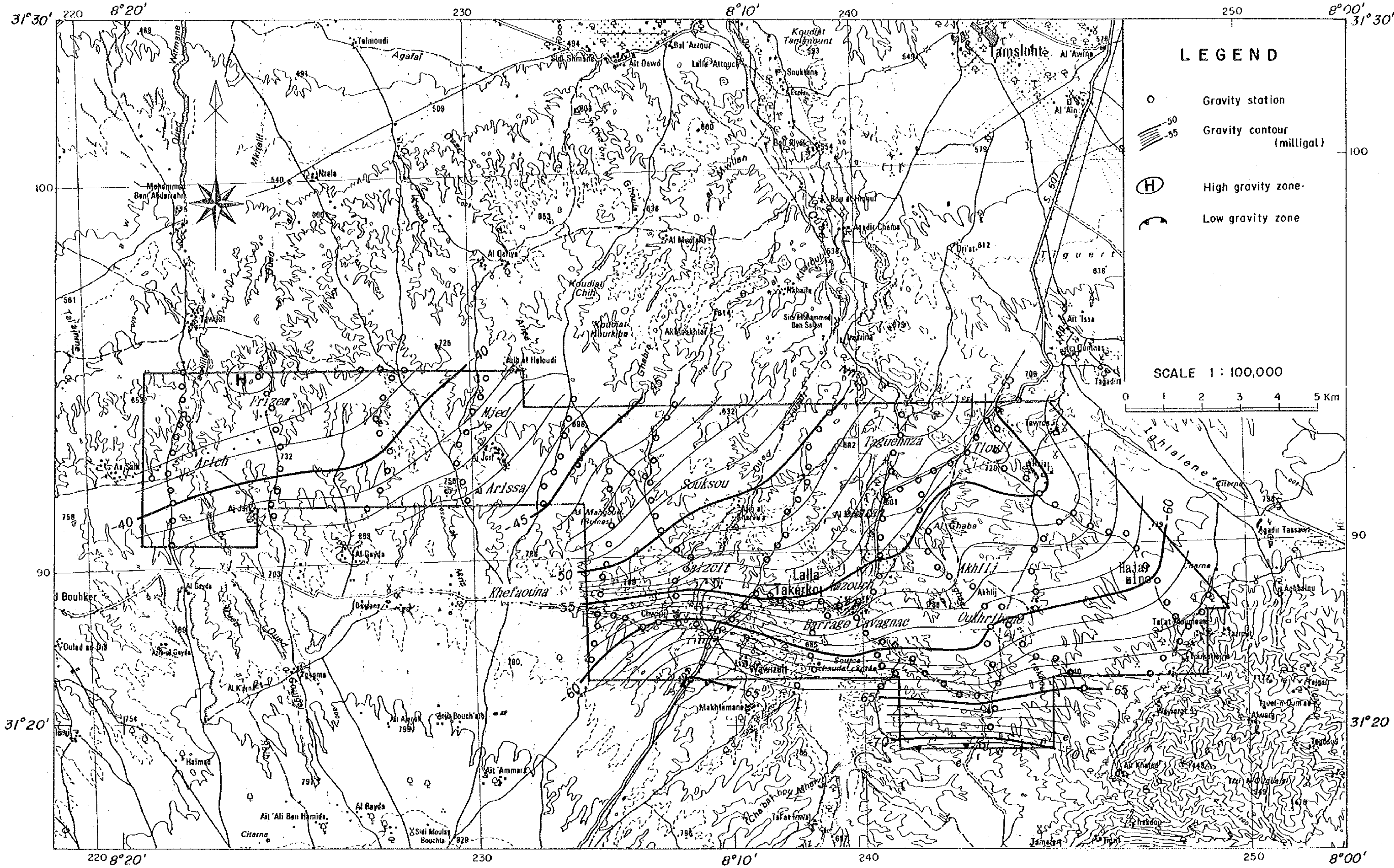

Fig. II-22 Bouguer Anomalies

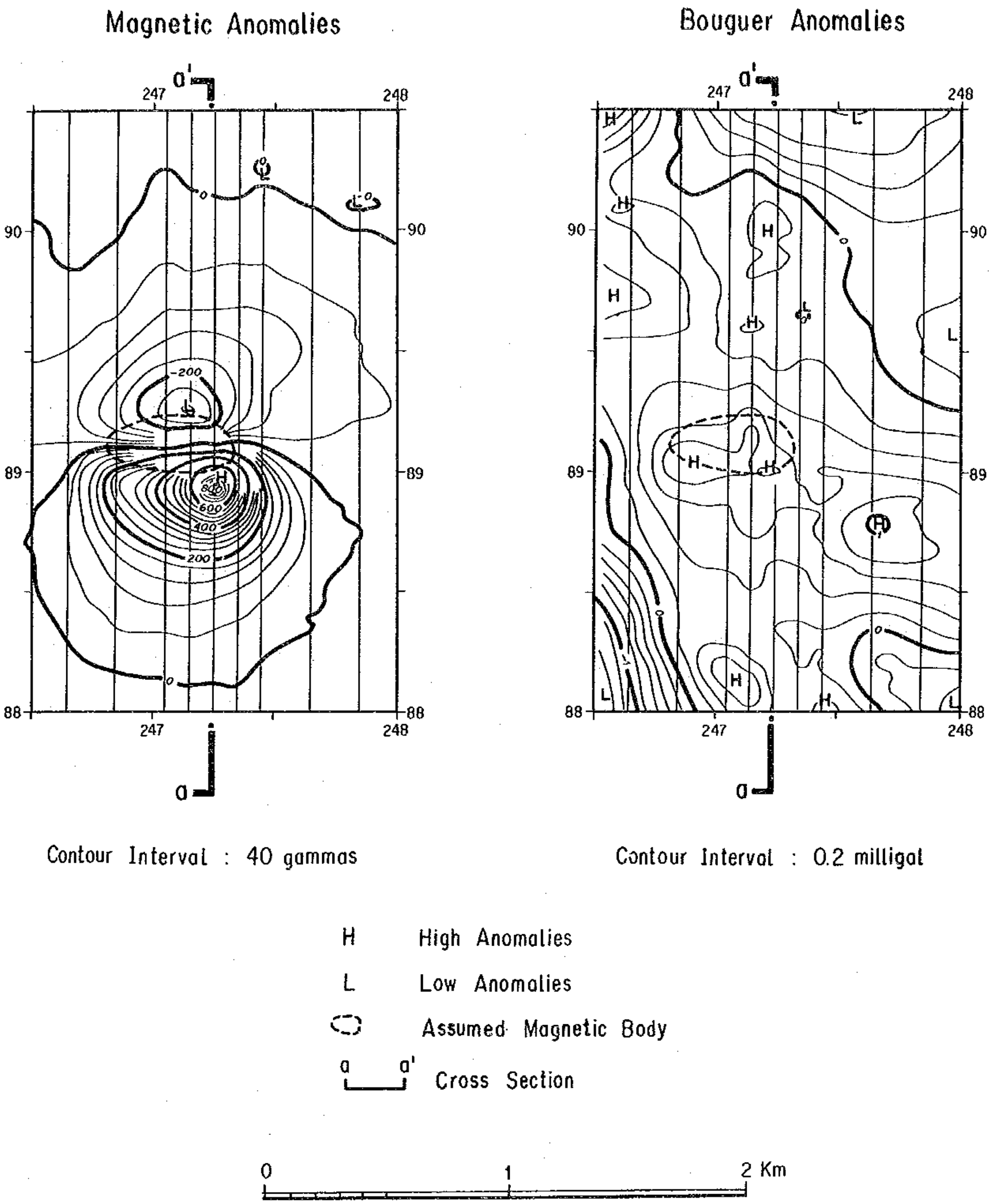

Fig. II-23 Detailed Geophysical Survey over Hajar Mine

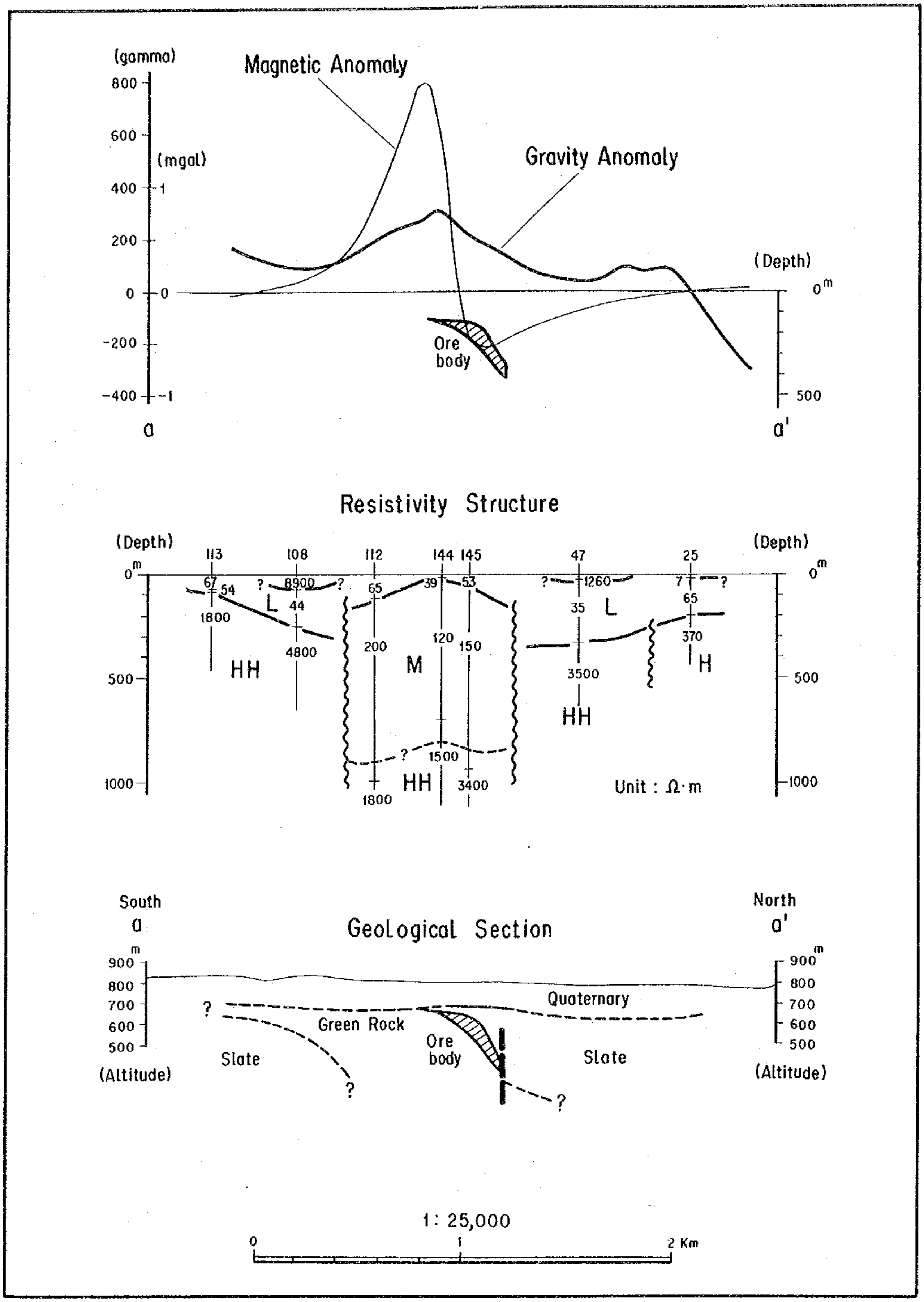

Fig. II-24 Comparison of Geophysical Survey over Hajar Mine

【REFERENCES】

1. Banno,S. and Seki,y. (1978) : Thermodynamics Analysis about Metamorphism, Geochemistry of Rocks and Minerals, Earth Science 4, Iwanami, p.191-240 (in Japanese).
2. Banno,S. (1979) : Malti-phase System and Equivalent, Geochemistry of Rocks and Minerals, Earth Science 4, Iwanami, p.147-165 (in Japanese).
3. BRGM (1985) : Carte Géologique Provisoire du Massif des Guemassa, 1/50,000, BRPM.
4. BRGM/DG (1986) : Etude Géologique, Géochimique et Géophysique des Indices de Amzourh (Guemassa).
5. BRPM (1985) : Travaux Géophysiques Réalises à Douar El Hajar
6. Geoterrex Ltd. (1968) : Carte Résiduelle du Champ Magnétique Total, Zone 3, Seuil de Guemassa, 1/50,000, Direction des Mines et de la Géologie.
7. Geoterrex Ltd. (1968) : Prospection Electromagnétique Aérienne par Méthode Input Barringer sur les Extensions du District de Pyrrhotine des Jebilets, Ministère du Commerce, de L' Artisanat de L' Industrie & des Mines.
8. Goldstein,M.A. and Strangway,D.W. (1975) : Audio-frequency Magnetotellurics with a Grounded Electric Dipole Source, Geophysics,v.40,n.4,p.669-683.
9. Hunting Geology and Geophysics Ltd. (1968) : Helicopter-borne GeophysicalProject, BRPM and Arab Mining Company.
10. Maier,w., Mellal, and El Hakour,A. (1986) : Le Gisement Polimétallique Hydrothermal-Sédimentaire de Douar Lahjar, BRPM.
11. Ministère du Commerce (1970) : Carte Géologique et des Minéralisations des Jebilet Centrales, 1/100,000, reviewed by P.Huvelin.
12. Ministère de L' Energie et des Mines : Gravimétrie Haouz, Anomalie de Bouguer, d = 2.2.

13. Ministere de L' Energie et des Mines (1982) : Carte Géologique du Maroc , 1/1.000.000 .

14. Sawa.K. and Yairi.K. (1979) : Geology of Africa. Geology of the World. Earth Science 16. Iwanami. p.61-98 (in Japanese) .

15. Yamashita.M. (1984) : CSAMT Controlled Source Audio Magnetotellurics. Phoenix Geophysics Ltd.

APPENDICES

AP. I — 1 List of Rock and Ore Samples

(1)

No.	Sample No.	Type of Sample	Geol. Unit	Location	Kind of Analysis				
					T	P	X	R	O
1	29	Quartz vein	V	W-Ar		P			O
2	58	Gabbro	Gb	W-Ka	T			R	
3	60	Limestone	Il	W-Mj	T				
4	66	Rhyolite	Ry	W-Ka	T				
5	103	Pel sch	Ips	W-Nz			X	R	
6	106	Calc sch	Ic	W-Mj			X		
7	109	Calc sch	Ip	W-Ka				R	
8	118	Porphyrite	Pr	W-Mk	T				
9	120	Gossan	Ic	W-Mk		P			
10	121	Gabbro	Gb	W-Nz	T				
11	124	Quartz vein	V	W-Nz		P			
12	132	Calc sch	Ipm	W-Mk			X	R	
13	134	Pel sch	Ic	W-Mk			X	R	
14	138	Pel sch	Ips	W-Ar				R	
15	145	Diorite	Dr	W-Ar	T				
16	167	Diorite	Dr	W-Mj	T				
17	175	Calc sch	Ic	W-Mj			X		
18	183	Rhyolite	Ry	W-Fr			X	R	
19	187	Rhyolite	Ry	W-Fr	T				
20	215	Calc sch	Ic	W-Da			X	R	
21	242	Pel sch	Ic	W-Mk			X	R	
22	258	Pel sch	Ip	W-Ka			X		
23	301	Green rock	IIat	E-Ha	T		X	R	
24	302	Low-grade ore	or	E-Ha	T	P	X	R	O
25	303	High-grade ore	or	E-Ha		P			O
26	304	Pyrrhotite	or	E-Ha					O
27	306	Diss ore	or	E-Ha		P			O
28	307	Green rock	IIat	E-Ha	T		X	R	
29	309	Low-grade ore	or	E-Ha	T				
30	310	High-grade ore	or	E-Ha					O
31	313	Meta rhyolite	IIav	E-Am	T		X	R	
32	317	Green rock	IIat	E-Am	T		X	R	
33	322	Diorite	D	E-Am	T			R	
34	323	Slate	IIpl	E-Am			X	R	

No.	Sample No.	Type of Sample	Geol. Unit	Location	Kind of Analysis				
					T	P	X	R	O
35	326	Gossan	IIas	E-Ou					O
36	327	Gossan	IIas	E-Ou		P	X		O
37	328	Slate	IIas	E-Ou				R	
38	334	Gossan	IIat	E-Ou		P			O
39	335	Gossan	IIat	E-Ou		P	X		O
40	336	Green rock	IIat	E-Ou	T		X	R	
41	338	Limestone	IIp2	E-Ak	T				
42	340	Limestone	IIp2	E-Ak			X		
43	360	Calc semischist	IIc	E-Im	T		X	R	
44	367	Rhyolite	Ry	E-Im	T			R	
45	372	Rhyolite	Ry	E-Ak	T				
46	401	Quartz vein	V	W-Nz		P			

Abbreviation

Calc sch : Calcareous schist
Diss : Dissemination
Pel sch : Pelitic schist

T : Thin Section
P : Polished Section
X : X-ray Analysis
R : Whole Rock Analysis
O : Ore Assay

Ak : Akhlij
Am : Amzourh
Ar : Arich
Da : Daoud
E : Eastern area
Fr : Frizem
Ha : Hajar

Im : Imarine
Ka : Karia
Mj : Mjed
Mk : Mkhatif
Nz : Nzala
Ou : Oukhribane
W : Western area

AP. I — 2 Assay Results of Ore Samples

No.	Sample No.	Type of Sample	Grade			
			Ag(g/t)	Cu(%)	Pb(%)	Zn(%)
1	29	Quartz vein	14.0	0.04	1.65	2.28
2	302	Low-grade ore	54.0	1.82	3.90	12.20
3	303	High-grade ore	128.0	3.20	12.00	18.00
4	304	Pyrrhotite	34.0	4.40	1.00	13.20
5	306	Dissemination ore	3.2	3.10	0.06	1.00
6	310	High-grade ore	7.6	4.30	0.44	10.00
7	326	Gossan	3.2	1.08	0.92	1.52
8	327	Gossan	1.6	1.18	0.07	1.60
9	334	Gossan	2.8	0.42	0.02	0.38
10	335	Gossan	1.2	0.66	0.12	0.12

AP. I－3 Whole Rock Analysis and Molal Ratio

(1)

Sample Rock	103 Pel	132 Calc	134 Pel	138 Pel	215 Calc	242 Pel	323 Slate	328 Slate	109 Calc	360 Calc
SiO2	60.72	60.90	58.31	63.93	63.50	62.92	62.99	56.97	57.89	61.39
TiO2	0.79	0.57	0.93	0.69	0.75	0.77	0.87	0.96	0.83	0.32
Al2O3	17.99	12.34	21.35	17.72	17.61	18.09	17.84	19.60	18.44	7.43
Fe2O3	1.43	2.19	1.23	1.26	1.77	1.57	1.13	2.62	3.45	0.06
FeO	4.58	2.28	4.28	3.96	4.16	4.91	4.64	5.20	4.55	3.04
MnO	0.13	0.10	0.03	0.06	0.07	0.06	0.07	0.06	0.11	0.05
MgO	2.03	1.32	2.31	1.66	1.97	2.16	1.81	3.04	2.42	1.77
CaO	1.59	7.94	0.62	0.62	0.68	0.40	0.87	0.70	1.43	12.92
Na2O	1.27	0.20	0.26	1.54	0.15	0.76	0.55	0.10	1.51	0.99
K2O	3.18	2.58	4.62	3.56	3.95	3.17	4.13	3.14	2.87	1.57
P2O5	0.08	0.10	0.18	0.06	0.14	0.14	0.10	0.14	0.17	0.06
LOI	5.26	8.63	4.97	4.00	4.31	4.25	4.44	6.73	5.40	9.74
Total	99.05	99.15	99.09	99.06	99.06	99.20	99.44	99.16	99.07	99.34
SiO2	1.0106	1.0136	0.9705	1.0640	1.0568	1.0472	1.0484	0.9482	0.9635	1.0217
TiO2	0.0099	0.0071	0.0116	0.0086	0.0094	0.0096	0.0109	0.0120	0.0104	0.0040
Al2O3	0.1764	0.1210	0.2094	0.1738	0.1727	0.1774	0.1750	0.1922	0.1809	0.0729
Fe2O3	0.0090	0.0137	0.0077	0.0079	0.0111	0.0098	0.0071	0.0158	0.0216	0.0004
FeO	0.0637	0.0317	0.0596	0.0551	0.0579	0.0683	0.0646	0.0724	0.0633	0.0423
MnO	0.0018	0.0014	0.0004	0.0008	0.0010	0.0008	0.0010	0.0008	0.0016	0.0007
MgO	0.0504	0.0328	0.0573	0.0412	0.0489	0.0536	0.0449	0.0754	0.0600	0.0439
CaO	0.0284	0.1416	0.0111	0.0111	0.0121	0.0071	0.0155	0.0125	0.0255	0.2304
Na2O	0.0205	0.0032	0.0042	0.0248	0.0024	0.0123	0.0089	0.0016	0.0244	0.0160
K2O	0.0338	0.0274	0.0490	0.0378	0.0419	0.0337	0.0438	0.0333	0.0305	0.0167
P2O5	0.0006	0.0007	0.0013	0.0004	0.0010	0.0010	0.0007	0.0010	0.0012	0.0004
A	0.05467	0.03563	0.05805	0.03556	0.04449	0.06419	0.03456	0.09061	0.06508	0.00689
F	0.06374	0.03173	0.05957	0.05511	0.05790	0.06834	0.06458	0.07237	0.06332	0.04231
M	0.05036	0.03275	0.05731	0.04118	0.04887	0.05359	0.04490	0.07542	0.06004	0.04391
A	0.02206	0.01720	0.02466	0.00804	0.01398	0.02936	0.00327	0.04838	0.02983	-0.0177
C	0.02835	0.14159	0.01105	0.01105	0.01212	0.00713	0.01551	0.01248	0.02550	0.23039
F	0.00895	0.01371	0.00770	0.00789	0.01108	0.00983	0.00707	0.01578	0.02160	0.00037

(2)

Sample Rock	183 Rhyolite	313 Rhyolite	367 Rhyolite	322 Diorite	301 Green	307 Green	317 Green	336 Green	58 Gabbro	302 Ore
SiO2	77.28	76.43	80.04	71.37	52.75	55.32	76.42	56.70	45.24	23.16
TiO2	0.13	0.34	0.14	0.24	1.02	0.67	0.47	0.87	0.80	0.03
Al2O3	10.13	12.25	11.69	14.67	22.27	12.64	9.04	17.50	15.09	4.85
Fe2O3	2.06	0.67	0.01	1.54	2.16	0.96	0.61	5.58	0.24	10.82
FeO	1.05	1.63	0.93	1.52	5.57	16.16	6.45	5.35	8.90	14.64
MnO	0.02	0.08	0.01	0.15	0.16	0.28	0.14	0.18	0.15	0.25
MgO	0.23	0.36	0.21	0.49	3.46	7.71	1.63	2.29	12.83	14.84
CaO	0.09	0.93	0.43	0.37	0.35	0.05	0.26	0.89	9.09	0.10
Na2O	0.19	0.11	3.04	2.85	0.67	0.01	0.06	0.17	1.85	0.03
K2O	3.10	3.96	1.61	3.25	5.76	0.01	1.42	6.10	0.45	0.02
P2O5	0.08	0.27	0.04	0.05	0.15	0.02	0.08	0.10	0.12	0.07
LOI	4.63	2.18	1.30	2.91	4.98	5.30	2.42	3.43	4.30	13.16
Total	98.99	99.21	99.45	99.41	99.30	99.13	99.00	99.16	99.06	81.97
SiO2	1.2862	1.2720	1.3321	1.1878	0.8779	0.9207	1.2719	0.9437	0.7529	0.3855
TiO2	0.0016	0.0043	0.0018	0.0030	0.0128	0.0084	0.0059	0.0109	0.0100	0.0004
Al2O3	0.0994	0.1201	0.1147	0.1439	0.2184	0.1240	0.0887	0.1716	0.1480	0.0476
Fe2O3	0.0129	0.0042	0.0001	0.0096	0.0135	0.0060	0.0038	0.0349	0.0015	0.0678
FeO	0.0146	0.0227	0.0129	0.0212	0.0775	0.2249	0.0898	0.0745	0.1239	0.2038
MnO	0.0003	0.0011	0.0001	0.0021	0.0023	0.0039	0.0020	0.0025	0.0021	0.0035
MgO	0.0057	0.0089	0.0052	0.0122	0.0858	0.1913	0.0404	0.0568	0.3183	0.3682
CaO	0.0016	0.0166	0.0077	0.0066	0.0062	0.0009	0.0046	0.0159	0.1621	0.0018
Na2O	0.0031	0.0018	0.0490	0.0460	0.0108	0.0002	0.0010	0.0027	0.0298	0.0005
K2O	0.0329	0.0420	0.0171	0.0345	0.0611	0.0001	0.0151	0.0648	0.0048	0.0002
P2O5	0.0006	0.0019	0.0003	0.0004	0.0011	0.0001	0.0006	0.0007	0.0008	0.0005
A	-0.0024	-0.0077	0.01432	-0.0056	0.02415	0.12348	0.04246	-0.0253	0.10381	0.04644
F	0.01461	0.02268	0.01294	0.02115	0.07752	0.22492	0.08977	0.07446	0.12387	0.20376
M	0.00570	0.00893	0.00521	0.01215	0.08584	0.19129	0.04044	0.05681	0.31832	0.36819
A	-0.0082	-0.0167	0.00913	-0.0151	-0.0225	0.00456	0.00526	-0.0628	-0.0225	-0.1169
C	0.00160	0.01658	0.00766	0.00659	0.00624	0.00089	0.00463	0.01687	0.16209	0.00178
F	0.01289	0.00419	0.00006	0.00964	0.01352	0.00601	0.00381	0.03494	0.00150	0.06775

AP. I — 4 — 1 Microscopic Observation of Thin Sections (1)

No.	Sample No.	Rock Name	Texture	Location	Observed Minerals: Primary Minerals																		Secondary Minerals																			
					Quartz	Plagioclase	K-feldspar	Biotite	Hornblende,	Clinopyroxene	Orthopyroxene	Magnetite	Apatite	Olivine	Nontronite	Chlorite	Calcite	Zircon	Hematite	Dolomite	Sphene	Opaque minerals	Quartz	Carbonate	Calcite	Clinopyroxene	Epidote	Chlorite	Galnet	Sericite	Biotite	Amphibole	Hematite	Nontronite	Sphene	Goethite	Smectite	Stilpnomelane	Sphalerite	Muscovite	Albite	Opaque minerals
1	58	Gabbro	Ophitic	W - Ka		4		3	3			3							2	4				2	3		2	3		2		4										
2	60	Dolomitic limestone	Fng granular	W - Mj	3			2																				1								1						
3	66	Meta rhyolite	Portic granular	W - Ka	3	3		3					1												3			3		4								2				
4	118	Porphyry	Portic holocryst	W - Mk	3	4	3					2	2										3	3	4		1	3			3											
5	121	Olivine basalt	Porphyritic	W - Nz	2	4						2	3	4	4	4	4								3			4			2		2	4								
6	145	Porphyry	Portic holocryst	W - Ar	3	4	3	3		3	3	2													3			3		2					2	2						
7	167	Porphyry	Portic holocryst	W - Mj	3	3	3	2		3	3	2	3					1							3			3							2		3					
8	187	Meta rhyolite	Mosaic	W - Fr	4	3						2						1										3		4			2	3		2						
9	301	Meta siltstone	Fine-grained	E - Ha	3	2												1										2		4												3
10	302	Chlorite schist	Schistoze	E - Ha																								4											3	3		4
11	307	Meta mudstone	Granular	E - Ha	4	3	2											1										4			3				2							2
12	309	Chlorite schist	Schistoze	E - Ha																			3	3				4													3	3
13	313	Meta rhyorite	Gran, grading	E - Am	4	3																		3						4	2		1									2
14	317	Meta siltstone	Granular	E - Am	4																							3		3	3										3	
15	322	Meta dolerite	Porphyritic	E - Am	3	4	4																	2							3			4								
16	336	Biotite schist	Gran weak foliation	E - Ou	4																			2						4	4			4								1
17	338	Bt-ser semisch	Spotted	E - Ak	3	2																						3		4	4		1		1							
18	360	Cal-qz semisch	Granular	E - Im	4	3	2																		4						4		1		1							
19	367	Meta rhyorite	Porphyritic	E - Im	3	3	3						1							1		1	2		3			1		4												
20	372	Meta rhyorite	Granular	E - Ak	4	3												1										2		4						1						1

4 : Abundant   3 : Common   2 : Little   1 : Rare

58 : Gabbro

The rock shows ophitic texture. Larger crystals are plagioclase, hornblende and magnetite. The former two minerals reaches 5 mm in size. Plagioclase is partly altered to sericite, carbonate and actinolite. Hornblende forms ophitic plate with plagiocase laths and are mantled with actinolite. Magnetite is smaller than 1 mm across and is altered to sphene and carbonate. Plagioclase laths and minor biotite and magnetite fill the interstices of larger crystals mentioned above. Secondary minerals are abundant acicular actinolite, less abundant calcite, chlorite and minor sericite, carbonate and rare clinozoisite.

60 : Dolomitic limestone

The rock has granular texture. The major components are dolomite and quartz, ranging 0.2 to 2 mm and 0.5 mm or less in diameter, respectively. The minor components are muscovite and hematite. Secondary chlorite and goethite are very small in amount.

66 : Meta rhyolite

The rock shows porphyritic texture. Phenocrysts are plagioclase, pyroxene, apatite and muscovite. Plagioclase phenocrysts are smaller than 1 mm and are altered to aggregates of smectite, calcite and goethite. Apatite phenocrysts have long or stout prismatic forms up to 2 mm long. The groundmass is constituted by quartz, plagioclase, potash feldspar, biotite, magnetite and accessory zircon. Secondary minerals are calcite, chlorite, smectite, goethite and sphene.

118 : Carbonatized porphyry

The rock shows porphyritic texture. Phenocrysts are plagioclase, magnetite and pyroxene. Plagioclase phenocrysts are up to 2 mm in size, and are twinned. They are partly altered to calcite and clinozoisite. Magnetite phenocrysts are smaller in amount and size, under 0.2 mm. Pyroxene phenocrysts, smaller than 1 mm, are completely replaced by aggregates of chlorite, carbonate and smectite. The groundmass is holocrystalline and consists of quartz, plagioclase, alkali feldspar, magnetite and apatite and secondary biotite.

121 : Olivine basalt

The rock is porphyritic with abundant olivine and apatite phenocrysts and rare plagioclase and magnetite phenocrysts. Olivine phenocrysts have prismatic, up to 1 mm long, or granular and are completely altered to nontronite, chlorite and calcite aggregates. Plagioclase phenocrysts are characterized by noted marginal zoning without twinning. Magnetite phenocrysts are smaller than 0.3 mm and are replaced by hematite. The groundmass is made up of plagioclase laths, altered olivine and sporadic interstitial quartz.

145 : Porphyry

The rock is porphyritic with plagioclase, pyroxene and magnetite phenocrysts. Plagioclase phenocrysts are up to 2 mm and show noted marginal zoning. They are partly altered to carbonate and sericite. Pyroxene phenocrysts, up to 2 mm in size, are thoroughly replaced by aggregate of chlorite, opaque mineral, calcite and sphene. Magnetite phenocryts are smaller than 0.5 mm and are altered partly to hematite and sphene. The groundmass is composed of plagioclase, potash feldspar, quartz, biotite, altered pyroxene and magnetite. Secondary chlorite and goethite are present sporadically.

167 : Carbonatized porphyry

The rock has porphyritic texture. Phenocrysts are plagioclase, pyroxene, apatite and biotite. Plagioclase phenocrysts are smaller than 1 mm. Pyroxene phenocrysts attain 2 mm in length and are altered to smectite, calcite and goethite. Apatite phenocrysts are long or stout prismatic, up to 2 mm long. Biotite phenocrysts are 1 mm or less in size. The groundmass is holocrystalline and consists of quartz, plagioclase, potash feldspar, biotite, magnetite and rare zircon with secondary chlorite.

187 : Meta rhyolite

The rock shows mosaic texture, Main constituent minerals are quartz, plagioclase and magnetite, Quartz grains are up to 1 mm in diameter. Plagioclase grains are also up to 1 mm, with zonal structure and twinning. Magnetite grains, smaller than 0.5 mm, show ragged outline and alteration to hematite. Assessory mineral is zircon. Secondary sericite, chlorite, nontronite, hematite and goethite are ubiquitous.

301 : Meta siltstone

The rock is fine-grained. Clastic grains are quartz, plagioclase and rare zircon. Quartz and plagioclase grains are both smaller than 0.2 mm across, the latter being less in amount. Zircon grains are smaller than 0.1 mm. Secondary minerals are sericite, opaque mineral and chlorite. Sericite is abundant. Opaque mineral occurs as irregular, ragged veins.

302 : Chlorite schist

The rock shows schistose texture. Schistosity is constructed by leucocratic and melanocratic bands. The leucocratic bands consist of curved flaky chlorite and muscovite. The melanocratic bands are made of granular grains of spharelite and irregular opaque mineral, the former being inside the latter.

307 : Meta mudstone

The rock shows granular texture, consisting of abundant quartz grains. Main components of grains are quartz, plagioclase with less potash feldpar and rare zircon. All the grains are smaller than 0.1 mm across. Secondary minerals are chlorite, biotite, opaque mineral and sphene.

309 : Chlorite schist

The rock has schistose texture. Schistosity is constructed by abundant chlorite in preferred orientation. The other componts of the rock are quartz, opaque mineral, albite and carbonate. Quartz occurs as grains with ragged outline. Opaque mineral has irregular forms.

313 : Meta rhyorite

The rock shows granular texture with weak bedding and grading. The main constituents are quartz and plagioclase. Both the minerals are sometimes up to 1 mm across, but usually smaller than 0.01 mm across. Plagioclase is replaced by carbonate. Secondary minerals are abundant flaky sericite, less abundant carbonate, and minor biotite and opaque mineral and accessory hematite.

317 : Meta siltstone

The rock has granular texture. The granules are exclusively quartz. Quartz grains are smaller than 0.1 mm across and have ragged outlines. Secondary minerals are muscovite, chlorite, biotite, albite, opaque mineral and rare goethite. Muscovite and biotite are arranged in preferred orientation.

322 : Meta dolerite

The rock shows porphyritic texture. Phenocrysts are plagioclase, potash feldspar and quartz. Plagioclase and potash feldspar phenocrysts are abundant and up to 1.5 and 1 mm in size, respectively. Quartz phenocrysts are less abundant and have ragged outlines. The most abundant secondary mineral is nontronite. And minor secondary minerals are biotite and carbonate.

336 : Biotite schist

The rock has granular texture with weak foliation. Granular texure is due to abundant occurrence of quartz grains smaller than 0.04 mm across. Sericite and biotite are major secondary minerals. Carbonate is minor and opaque mineral and hematite are accessory secondary minerals.

338 : Biotite-sericite semischist

The rock is spotted with biotite up to 0.4 mm in granular matrix consisting of quartz and plagioclase grains. Secondary minerals are spotted biotite, flaky sericite, minor chlorite, accessory hematite and sphene.

360 : Calcite-quartz semischist

The rock shows granular texture. Granular grains are mainly of quartz and less of plagioclase and potash feldspar. Quartz grains are up to 0.1 mm. Plagioclase and potash feldspar grains are both smaller than 0.1 mm across. Secondary minerals are biotite and calcite with rare grains of hematite and sphene.

367 : Meta rhyorite

The rock shows porphyritic texture. Phenocrysts are plagioclase up to 2 mm or more. The groundmass is holocrystalline and consists mainly of plagioclase, potash feldspar, quartz with very small amounts of sphene, opaque mineral and apatite. Secondary minerals are sericite, the most abundant, calcite and chlorite.

372 : Meta rhyorite

The rock has granular texture caused by arrangement of abundant quartz and less abundant plagioclase grains. Average grain sizes of the both minerals are 0.15 mm. Quartz grains up to 1.0 mm across are included frequently. Rarely zircon grains are present. Secondary minerals are predominantly sericite and accessory chlorite, opaque mineral and goethite.

AP. I—4—2 Microphotograph of Thin Sections

(1)

No.	Sample No.	Rock Name
(1), (2)	60	Dolomitic limestone
(3), (4)	121	Olivine basalt
(5), (6)	187	Meta rhyolite
(7), (8)	301	Meta siltstone
(9), (10)	313	Meta rhyolite
(11), (12)	317	Meta siltstone
(13), (14)	322	Meta dolerite
(15), (16)	336	Biotite schist

(Abbriviation)

Ap : apatite

Bi : biotite

Carb : carbonate minerals

Chl : chlorite

Dol : dolomite

Kf : potash feldspar

Ms : muscovite

Ov : olivine

Pl : plagioclase

Qz : quartz

Ser : sericite

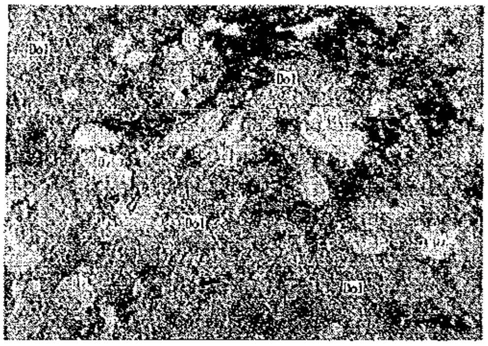

Plain polarized light 0 0.5mm

(1) 60

The major components are dolomite and quartz. They have granular texture.

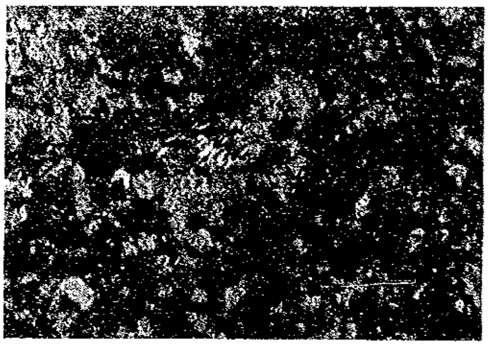

Crossed polarized light 0 0.5mm

(2) 60

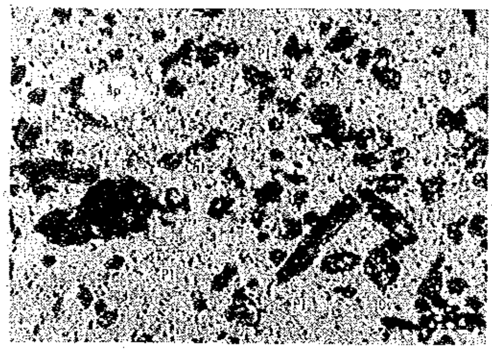

Plain polarized light 0 0.5mm

(3) 121

The rock is porphyritic with abundant olivine and apatite. The groundmass is made up of plagioclase laths and altered olivine.

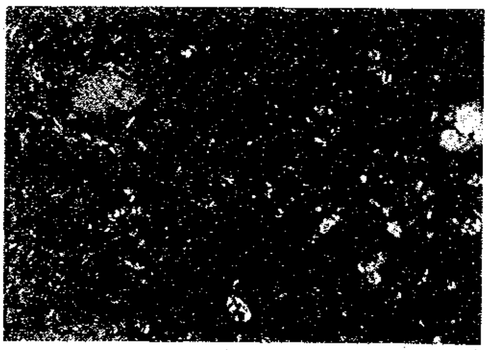

Crossed polarized light 0 0.5mm

(4) 121